Arctic bivalve dead-shell assemblages as high temporal- and spatial- resolution archives of ecological regime change in response to climate change

Caitlin A. Meadows[1]*, Jacqueline M. Grebmeier[2] and Susan M. Kidwell[1]

[1]Department of the Geophysical Sciences, The University of Chicago, 5734 S. Ellis Ave, Chicago, IL 60637, USA

[2]University of Maryland Center for Environmental Sciences, Chesapeake Biological Laboratory, 146 Williams Street, Solomons, MD 20688, USA

CAM, 0000-0003-4146-2634; JMG, 0000-0001-7624-3568; SMK, 0000-0001-5477-4157

*Correspondence: meadowsc@uchicago.edu

Abstract: A 15-year time-series of data on benthic community response to rapid climate change at a biomass 'hotspot' in the northern Bering Sea, Alaska, provides an exceptional opportunity to evaluate naturally occurring molluscan dead-shell assemblages as ecological archives. We find that, at five middle-shelf stations censused annually from 2000 to 2014, dead-shell assemblages collected in 2014 are dominated by obligate deposit-feeding Nuculanidae bivalves as opposed to the other families in that guild or the facultative deposit-feeding Tellinidae that dominate the most recent living bivalve assemblages, thus correctly detecting the location and direction of known ecological changes. However, live–dead contrast is significant where the bivalve biomass and abundance has declined over time, and muted where bivalve abundances, and therefore shell input, increased, underscoring the general danger of assuming constant shell input. We also find that proportional abundance-based measures are best suited for detecting benthic response to climate change. Combined with preliminary results from shell age-dating, these results indicate that dead-shell assemblages provide a short-lived but compositionally faithful ecological memory well-suited for detecting recent site- and habitat-level ecological change under cold-water conditions. With marine regime change suspected to now be underway throughout the Arctic, molluscan dead-shell assemblages should become an integral part of efforts to detect transitioning regions.

Death assemblages are the time-averaged accumulations of dead and discarded skeletal remains encountered in the surficial sedimentary record of a modern environment, representing input from past generations. If their composition has not been too biased by differential preservation or transport of species, then they have the potential to register ecological conditions over much longer periods than typically encompassed by biomonitoring and other observational data (for reviews, see Kidwell 2013; Kidwell and Tomašových 2013; Kowalewski *et al.* 2018). The fidelity – faithfulness – of marine molluscan death assemblage composition to that of local source communities has been tested many times in diverse settings by comparing the numerical abundance and richness of species and functional groups with counterpart information from living assemblages collected in the same samples. Meta-analysis of dozens of such 'live–dead' studies and modelling (summarized in Kidwell and Tomašových 2013) find in fact that live–dead agreement is typically very good in level-bottom subtidal settings with no history of human modification: live–dead differences can be attributed largely or entirely to the coarser temporal resolution of the death assemblage relative to a 'snapshot' of the living. Habitats yielding poor live–dead agreement by such measures as taxonomic similarity, species' rank-abundance, and strongly offset centroids in multivariate space are, in contrast, consistently from areas with known or suspected human activities, which have apparently shifted the living assemblage from its baseline state, which the time-averaged death assemblage remembers (Kidwell 2007). The strong association of live–dead discordance with anthropogenic stressors, and not simply with settings of high natural variability, recommends including death assemblages in protocols for environmental assessment, using dead-only and live-only species (or species with strongly disparate live and dead abundances) as indicators of recent declines and arrivals (Kidwell 2007). Extensive field studies by geologists have used such live–dead discordance to confirm or resolve habitat-level biological responses to suspected human activities such as eutrophication, species invasion, and fishing (Staff and Powell 1999; Ferguson 2008; Chiba and Sato 2013; Gallmetzer *et al.* 2017), and to detect community shifts of uncertain or compounded

From: Nawrot, R., Dominici, S., Tomašových, A. and Zuschin, M. (eds) *Conservation Palaeobiology of Marine Ecosystems*. Geological Society, London, Special Publications, **529**,
https://doi.org/10.1144/SP529-2022-131

sources (Weber and Zuschin 2013; Arkle and Miller 2018; Michelson *et al.* 2018; Haselmair *et al.* 2021; Gilad *et al.* 2018).

Here, we assess the power of live–dead discordance to detect a known community-level benthic response to climate change in the Alaskan Arctic, which is undergoing especially rapid physical and biological changes both on land and under the sea (Johannessen *et al.* 2004). Marine climate change is more insidious – i.e. creeping and pervasive – than point-source stressors, such as wastewater outfalls, and is less direct than dredge-spoil dumping and trawling, and should thus be more challenging to detect using live–dead comparison (but see the successful single-taxon analysis by Powell *et al.* 2017). Arctic seabeds should also, in principle, present especially difficult postmortem conditions for preservation of biogenic carbonate. In addition to intensive bioturbation and aerobic decomposition of organics that promote acid production in porewaters everywhere, overlying cold waters pose an additional well-appreciated preservational barrier because of the sensitivity of the aragonite saturation state to temperature, creating a strong latitudinal gradient in the potential for carbonate dissolution (Jiang *et al.* 2015; Keil 2017). These conditions should act against the long-term accumulation of molluscan shells in Arctic subtidal seabeds, shortening the scale of time-averaging and, perhaps, intensifying the net biasing effects of shell loss on death assemblage composition by filtering out fragile shells more completely.

To evaluate these hypothesized effects, we analyse live–dead agreement within a 'hotspot' of macrobenthic biomass in the northern Bering Sea having an exceptional, 15-year time-series of benthic sampling: bivalve dead-shell assemblages retained from samples collected in the final year (2014) of this series could be compared against a known recent history of community composition. This study area is part of the Distributed Biological Observatory (DBO), an international observation network organized to co-ordinate analysis of biophysical responses to persistent sea ice loss and climate change across 10° of latitude in the Pacific Arctic (Moore and Grebmeier 2018). Annual summer cruises have tracked ocean chemistry, circulation, seabed conditions (organic and nutrient flux, sediment grain size), and biological communities across this broad region starting at various times in the 1990s, augmented with data from cruises in the 1970s and 1980s (Grebmeier 2012; Grebmeier *et al.* 2015*a*, 2018). Biophysical time-series data have revealed a strong coupling between physical oceanography, primary productivity, and the infaunal macrobenthic community. Macrobenthic communities in each of the DBO hotspots are maintained by organic matter produced along the thawing ice edge and in persistently ice-free areas such as polynyas (Grebmeier *et al.* 2015*a*). High primary productivity that starts with the spring thaw is accompanied by limited grazing owing to still-cold waters, and thus a large magnitude of primary productivity can reach shallow shelf seabeds; lateral, northward advection of part of that carbon can further feed the DBO regions, supporting extensive macrobenthic communities (Grebmeier 2012; Blanchard and Feder 2014; Mathis *et al.* 2014). Macrobenthic communities in the DBOs thus display strong pelagic-benthic coupling, i.e. from primary production in surface waters to seafloor biomass, and these macrobenthos serve, in turn, as food for benthivore mammals and seabirds; changes in organic delivery can thus cascade strongly from prey to predators (Grebmeier *et al.* 2015*a*; Lovvorn *et al.* 2018).

From this co-ordinated research, an ecosystem-wide marine 'regime change' was recognized in the northern Bering Sea occurring between 1990 and 2010, associated with the northward retreat of cold bottom waters and sea-ice (Grebmeier *et al.* 2006). Regime change in the northern Bering Sea consisted of decreases in planktic–benthic flux, decreased bottom current strength, and significant declines in total macrobenthic biomass, as well as a guild-level shift in dominance from obligate deposit feeders to facultative deposit (mixed suspension-deposit) feeders (trends described in Grebmeier *et al.* 2006, 2018).

As elsewhere in the Arctic, climate warming in the northern Bering Sea has thus been multifactorial, not simply a matter of warming temperature, making biotic effects difficult to predict from temperature alone (e.g. Saupe *et al.* 2014). In the marine realm, changes in minimum rather than mean or maximum temperature, temperature variability, oxygenation, nutrient upwelling and runoff, organic flux, and sediment grain size related to current strength can all have greater effects on benthic community composition than the more easily acquired data on mean temperature. These challenges place a premium on acquiring local empirical data on community composition from natural archives of ecological history such as dead-shell assemblages.

We previously evaluated the power of live–dead analysis for historical ecology using four biomonitored biomass hotspots throughout the northern Bering–Chukchi Sea system (DBO1–DBO4; Meadows *et al.* 2019). Each hotspot served as a separate region, distinguished by its relative stability and productivity, but we used only a single year of live data (standard protocol of live–dead analysis) and, to maximize comparability to ecosystem analysis, we used functional guilds and families rather than fine-, species- or genus-level taxa to characterize assemblage composition; moreover, we focused on

biomass as the unit of molluscan abundance. We found good live–dead agreement in hotspots of comparative stability, with significant live–dead discordance only in areas – or at individual sites within a hotspot – with documented changes in the composition of the living community, typically associated with changes in carbon delivery and/or sediment grain size.

Here we focus on site- and habitat-level variation within a single biomass hotspot in the northern Bering Sea (DBO1) using numerical abundance data exclusively (as is standard in live–dead analysis) and comparing dead-shell assemblages against the full historical dataset on living assemblage composition (2000–14) in order to test their archival quality more explicitly. Despite the aggressive high-latitude waters, we find (1) high spatial fidelity between live and dead shell assemblages, able to discern both site- and habitat-level changes in biological communities during the regime change, as well as (2) patterns consistent with high temporal resolution, i.e. a short-duration time-averaging compared to shelves at lower latitudes, likely owing to relatively lower rates of aragonite sequestration in the northern Bering Sea seabeds.

Study area

The DBO1 benthic-biomass hotspot in the northern Bering Sea is associated with a polynya (persistent ice-free area) just south of St Lawrence Island (Fig. 1), of critical importance historically to walrus and diving ducks. DBO1 was established in 2010 following time-series studies at 5 core sites starting in 1990, to monitor warming, with the expectation that 'subarctic' conditions would expand northward into the Bering Straits, replacing 'Arctic' conditions, which are characterized by colder and more nutrient-rich water, higher primary productivity, higher carbon export to seabeds, and, arising from these conditions, richer macrobenthic populations and benthivore predators (Grebmeier *et al.* 2018). The subarctic ecosystem is, in contrast, characterized by only seasonal ice cover, variable primary production, and generally lower benthic biomass. Between 1990 and 2000, the cold bottom water pool (<2°C) that had been maintained south of St Lawrence Island by seasonal sea ice started to retreat northward. This cold pool determined the position of the Arctic–subarctic boundary, with the cold water excluding subarctic taxa. With sea ice retreat, the southern extent of the cold pool boundary began fluctuating from year to year with greater variability (Mueter and Litzow 2008; Grebmeier *et al.* 2006, 2015*a*, *b*; Siddon 2021; Fig. 1). The subarctic ecosystem largely replaced Arctic conditions south of St Lawrence Island by the early 2010s (see sharp change in dates of sea ice break-up and freeze-up in Grebmeier *et al.* 2018, fig. 1b). The subarctic ecosystem has continued to expand northward into the southern Chukchi Sea, where it is now displacing Arctic conditions (Mueter and Litzow 2008; Grebmeier 2012; Siddon 2021).

We focus on data from five stations within DBO1 that were sampled annually between 2000 and 2014 (stations SLIP1-5 in Fig. 1; Table 1), the period when this hotspot was 'in transition'. In units of infaunal macrobenthic biomass, communities at DBO1 were highly productive in the early 2000s (*c.* 20 gC m^{-2}, ranging 10–30 gC m^{-2}), although punctuated by intense station-level changes interannually (Grebmeier 2012; Blanchard 2014; Grebmeier and Cooper 2016*b*). Biomass declined significantly toward 2015, an effect of interannual variability in the precise position of the cold bottom water pool and of the polynya, and a related slowing of north-flowing bottom currents, which allow particulate organic matter to settle to the seabed (Grebmeier 2012; Cross *et al.* 2018; Creamean *et al.* 2019). DBO1 stations were positioned along a gradient of organic flux created by these conditions, with increasing seafloor macroinvertebrate biomass to the north (SLIP4). The three stations in the southern area of the DBO1 are characterized by sandy mud (SLIP1–3), and two northern stations (SLIP4–5) are characterized by mud with <10% sand (Table 2).

The organic flux to DBO1 fed dense populations of benthic macrofauna, which in turn created bioturbated and thus well-aerated sediments (Table 2). Carbon dioxide from benthic respiration is thought to contribute to seasonally strong acidification of bottom waters in DBO1 (Emerson *et al.* 1990; Mathis *et al.* 2014; Cross *et al.* 2018). Thus, strong aragonite undersaturation of sedimentary porewaters is likely within DBO1; such seafloor chemistry would be antagonistic to the post-mortem persistence of shell carbonate. Destruction and damage to shells on such densely productive seafloors might also arise from bioturbation and the large populations of benthivorous birds and mammals (Cooper *et al.* 2013; Grebmeier *et al.* 2015*c*).

Methods

Variation in sediment type

For all sediment samples referenced in this study, sediment was collected from the first van Veen grab used for collection of sediment at sea, packaged in whirl-pak bags, and frozen for post-cruise analyses at land-based facilities. Sediment grain size was determined in the laboratory, normally (but not exclusively) after removal of organics and of iron oxides following the process of Gee and Bauder (1986). Sediment samples were acidified and

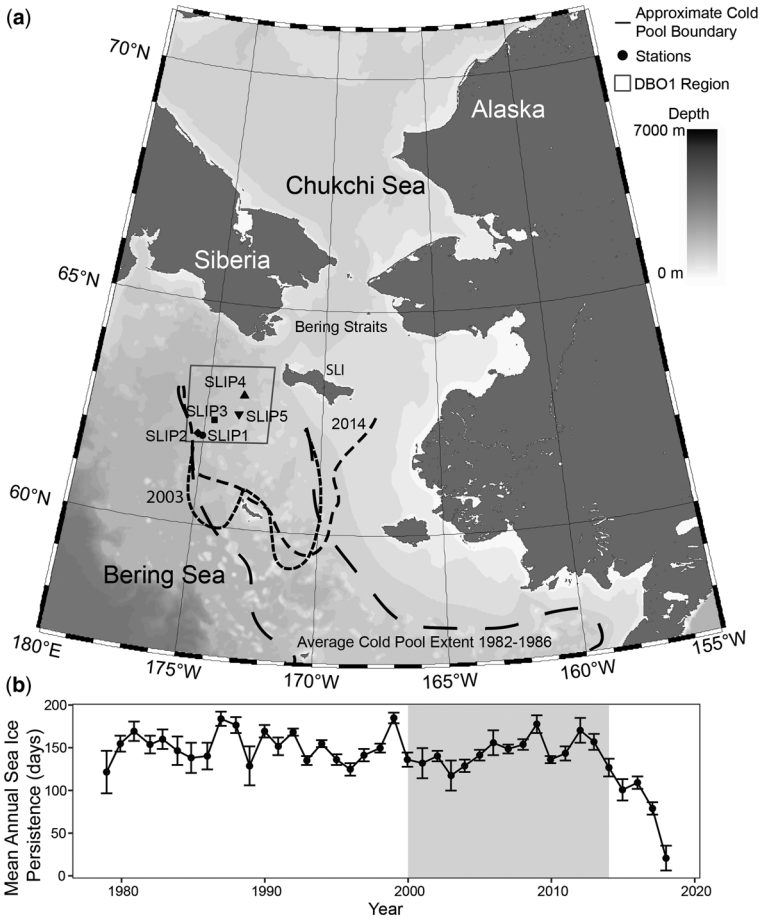

Fig. 1. (**a**) Study area in the North Pacific Arctic open continental shelf. Black icons denote stations (SLIP1–5) sampled for bivalve living and death assemblages from 2000 to 2014 within the northern Bering Sea Distributed Biological Observatory region 1 (DBO1, grey box). Dashed lines show the northward shift in the approximate southern limit of the cold bottom-water pool (<2°C) in the northern Bering Sea over the same period as the time-series examined here (Mueter and Litzow 2008; Siddon 2021). The DBO1 region is associated with a persistently ice-free polynya located south of St Lawrence Island (Grebmeier and Cooper 1995). Base map adapted from Ocean Data Viewer. (**b**) Sea ice persistence in the DBO1 region, using data from Grebmeier *et al.* (2018). Error bars depict spatial variability within the polygon of DBO1 region stations per year; grey band shows limits of the macrobenthic time-series used here.

provided to a land-based laboratory for carbon and nitrogen analyses at the University of California Santa Barbara in 1989–2008 and at the Nutrient Analytical Service Lab (NASL) of CBL in 2009–14. Methods of total organic carbon (TOC) and total organic nitrogen (TON) determination used one replicate (details of NASL methods are available at https://www.umces.edu/nasl/methods).

Stations within DBO1 can be separated into two sedimentary facies: three southern stations (sites) whose upper 0.5 cm is characterized by sandy mud (typically *c.* 70% mud, 24–35% sand, 'sandy mud'; SLIP1, SLIP2, SLIP3), and two northern stations characterized by less sand (85–90% mud, 'mud'; SLIP4, SLIP5 (Fig. 2a, Table 2; Grebmeier and Cooper 2016*a*, 2018, 2019*b*). At the sandy mud stations, mud content was relatively stable from 2000–04, somewhat variable over the next five years, and increased modestly from 2010–14 toward 90%, suggesting a slowing of currents (Fig. 2a), but this trend is not significant (Mann–Kendall trend test; $S = 0.104$, 0.109, 0.766 and all p-values $>>0.1$, for SLIP1, 2, and 3; Pohlert 2020). In contrast, mud content at both of the mud stations decreased slightly,

Table 1. *Data for each station used*

Ship	Station name	Latitude (°N)	Longitude (°W)	Sampling date	Water depth (m)	S Live bivalve families	Total live bivalve abundance (indiv./m^2)
LAU00	SLIP1	62.014	−175.057	20000719	80	6	652.5
LAU00	SLIP2	62.052	−175.208	20000719	80	5	612.5
LAU00	SLIP3	62.394	−174.587	20000719	71	5	610
LAU00	SLIP4	63.028	−173.458	20000720	70	7	542.5
LAU00	SLIP5	62.566	−173.553	20000720	65	6	2327.5
LAU01	SLIP1	62.013	−175.054	20010717	52	6	507.5
LAU01	SLIP2	62.050	−175.204	20010717	78	7	567.5
LAU01	SLIP3	62.394	−174.567	20010718	69	7	465
LAU01	SLIP4	63.025	−173.462	20010718	69	9	1035
LAU01	SLIP5	62.563	−173.555	20010718	62	7	2287.5
LAU02	SLIP1	62.011	−175.058	20020715	80	6	465
LAU02	SLIP2	62.050	−175.207	20020715	82	5	405
LAU02	SLIP3	62.392	−174.571	20020715	73	4	515
LAU02	SLIP4	63.031	−173.453	20020716	72	8	680
LAU02	SLIP5	62.562	−173.556	20020716	67	6	2097.5
LAU03	SLIP1	62.012	−175.055	20030714	84	8	577.5
LAU03	SLIP2	62.050	−175.213	20030714	84	6	677.5
LAU03	SLIP3	62.390	−174.571	20030715	72	7	465
LAU03	SLIP4	63.028	−173.456	20030715	73	6	725
LAU03	SLIP5	62.554	−173.563	20030715	67	6	2672.5
LAU04	SLIP1	62.013	−175.057	20040715	83	6	525
LAU04	SLIP2	62.054	−175.207	20040715	84	7	425
LAU04	SLIP3	62.393	−174.570	20040716	74	7	580
LAU04	SLIP4	63.028	−173.457	20040717	75	9	880
LAU04	SLIP5	62.563	−173.556	20040716	69	5	2037.5
LAU05	SLIP1	62.013	−175.054	20050714	83	5	695
LAU05	SLIP2	62.051	−175.204	20050715	83	7	645
LAU05	SLIP3	62.393	−174.570	20050715	73	6	975
LAU05	SLIP4	63.029	−173.458	20050716	73	7	1205
LAU05	SLIP5	62.563	−173.554	20050715	66	6	1692.5
LAU06	SLIP1	62.014	−175.054	20060712	80	6	695
LAU06	SLIP2	62.037	−175.218	20060712	82	6	957.5
LAU06	SLIP3	62.393	−174.570	20060713	73	5	670
LAU06	SLIP4	63.028	−173.458	20060713	73	8	1690
LAU06	SLIP5	62.566	−173.547	20060713	66	7	1165
LAU07	SLIP1	62.014	−175.057	20070714	80	7	1800
LAU07	SLIP2	62.051	−175.205	20070714	82	8	1205
LAU07	SLIP3	62.394	−174.569	20070714	67	6	537.5
LAU07	SLIP4	63.029	−173.457	20070714	36	8	2082.5
LAU07	SLIP5	62.563	−173.554	20070714	74	7	1870
LAU08	SLIP1	62.014	−175.056	20080716	80	5	852.5
LAU08	SLIP2	62.050	−175.205	20080716	83	5	867.5
LAU08	SLIP3	62.393	−174.570	20080716	73	7	432.5
LAU08	SLIP4	63.029	−173.458	20080717	73	8	1765
LAU08	SLIP5	62.564	−173.554	20080716	66	7	1355
LAU10	SLIP1	62.013	−175.050	20100716	86	7	250
LAU10	SLIP2	62.049	−175.200	20100716	83	6	207.5
LAU10	SLIP3	62.394	−174.569	20100716	73	6	275
LAU10	SLIP4	63.029	−173.458	20100717	73	8	1662.5
LAU10	SLIP5	62.562	−173.550	20100716	67	3	650
LAU11	SLIP1	62.010	−175.060	20110715	80	6	150
LAU11	SLIP2	62.050	−175.210	20110715	80	6	130
LAU11	SLIP3	62.390	−174.570	20110715	68	4	187.5
LAU11	SLIP4	63.030	−173.460	20110715	71	6	1472.5
LAU11	SLIP5	62.560	−173.551	20110715	65	4	662.5
LAU12	SLIP1	62.012	−175.066	20120714	80	5	445

(*Continued*)

Table 1. *Continued.*

Ship	Station name	Latitude (°N)	Longitude (°W)	Sampling date	Water depth (m)	S Live bivalve families	Total live bivalve abundance (indiv./m^2)
LAU12	SLIP2	62.050	−175.212	20120714	78	5	770
LAU12	SLIP3	62.390	−174.571	20120714	70	6	322.5
LAU12	SLIP4	63.030	−173.460	20120714	73	10	1092.5
LAU12	SLIP5	62.561	−173.551	20120714	62	4	450
LAU13	SLIP1	62.010	−175.060	20130713	80	7	710
LAU13	SLIP2	62.050	−175.210	20130713	81	6	587.5
LAU13	SLIP3	62.391	−174.571	20130714	73	7	440
LAU13	SLIP4	63.030	−173.460	20130714	73	10	1300
LAU13	SLIP5	62.560	−173.550	20130714	71	6	680

Samples with death assemblages

Ship	Station name	Latitude	Longitude	Sampling date	Water depth (m)	S Live bivalve taxa	Total live bivalve abundance (indiv./m^2)	D:L ratio	N Dead shells
LAU14	SLIP1	62.011	−175.059	20140714	81	8	725	5.17	1097
LAU14	SLIP2	62.050	−175.209	20140714	84	7	875	6.58	1712
LAU14	SLIP3	62.390	−174.570	20140714	71	8	460	6.41	876
LAU14	SLIP4	63.030	−173.460	20140714	65	9	1467.5	2.65	1156
LAU14	SLIP5	62.560	−173.549	20140715	71	6	617.5	4.90	905

Data include cruise name (Ship), latitude and longitude of sample, the sampling date (YYYYMMDD), water depth (m), gear used (all van Veen samplers; 3–5 grabs pooled per station), count of bivalve taxa (families) present as living individuals (*S*), the ratio of total dead individuals in the 2014 samples over the live abundance (indiv/m^2), and, for 2014 samples, the raw number of dead shells counted (*n* individuals).

converging toward the sandy mud stations, especially within the 2010–14 interval (Fig. 2a); these negative trends were also not significant (Mann–Kendall trend test; $S = -0.985$, 0.656, and all p-values $>>0.1$, for SLIP4 and 5; Pohlert 2020). Despite the (non-significant) trends toward similarity, two habitats remained distinct in grain size over the 15-year time-series using a Wilcoxon rank-sum test (% mud, $W = 36$, $p<<0.001$; R Core Team and Contributors Worldwide 2022). Qualitatively, grain sizes have been more variable at the sandy mud sites than at the mud sites.

The mud stations generally contain higher amounts of total organic carbon than the sandy mud seabeds, suggesting higher rates of carbon delivery; SLIP4 has the consistently highest TOC levels throughout the time-series (Fig. 2b). TOC has also generally increased and been more variable at the SLIP4 mud site than at any others (Fig. 2). When tested, no significant trends in TOC over time were detected at any station (Mann–Kendall trend test $S = -0.8$–0.16 with p-values $>>0.1$ for SLIP1-5). The two habitats remained distinct in TOC regime over the 15-year time-series using a Wilcoxon rank-sum test (TOC, $W = 240$, $p<<0.001$; R Core Team and Contributors Worldwide 2022).

Bivalve living assemblages

Living assemblages were sampled annually at SLIP1-5 between 2000 and 2014 by the Arctic Research Group (ARG; at the University of Maryland Centre for Environmental Science Chesapeake Biological Laboratory) using cruises of the Canadian Coast Guard Ship *Sir Wilfrid Laurier* (SWL or LAU; no cruise in 2009; Grebmeier *et al.* 2015*b*; Grebmeier and Cooper 2016*a*, 2018, 2019*a*, *b*). At each station, sediment and infauna were collected in the summer using two to five van Veen grabs (0.1 m^2, weighted with 32 kg to enhance penetration to 20–30 cm at these stations), sieved through a 1 mm screen with seawater, with the sieve residue preserved in 10% seawater-buffered formalin. van Veen grabs are commonly used for infaunal biomonitoring despite the likely under-sampling of deeply burrowing and large-bodied taxa (Munroe *et al.* 2013; Powell and Mann 2016; Powell *et al.* 2017; Mann *et al.* 2020). Processing using a 1 mm sieve has been standard for the ARG monitoring effort, as it is for many agency surveys (Gill *et al.* 2011; Becker 2015). At many sites within DBO shelf hotspots, Pirtle-Levy (2006) found that, on average, 97% of the station macrofaunal biomass was caught

Table 2. *Sediment characteristics of DBO1 stations from data collected as part of the PacMARS program from 2000 to 2012, along with with data from SWL cruises in 2013 and 2014*

Habitat	Station	Latitude (°N)	Longitude (°W)	Depth (m)	Sand (%)	Mud (%)	TOC (mg g^{-1})	TON (mg g^{-1})	C/N	SCOC (mmol O^2 m^{-2} d^{-1})
Sandy mud	SLIP1	62.01	−175.06	79	31.5 (26.5, 34.4)	68.5 (65.7, 73.5)	1.1 (1.0, 1.1)	0.17 (0.16, 0.18)	6.5 (6.1, 6.6)	8.29 (5.05, 9.39)
	SLIP2	62.05	−175.21	82	25.7 (23.5, 30.3)	74.3 (69.7, 76.4)	1.1 (1.0, 1.3)	0.18 (0.15, 0.20)	6.4 (6.2, 6.6)	9.55 (5.89, 12.82)
	SLIP3	62.39	−174.57	71	31.6 (26.7, 33.9)	68.3 (66.1, 73.3)	1.0 (0.8, 1.1)	0.16 (0.14, 0.18)	6.3 (6.0, 6.5)	11.47 (9.28, 13.03)
Mud	SLIP4	63.03	−173.46	69	4.9 (3.1, 7.2)	95.1 (92.8, 97.0)	1.7 (1.5, 1.7)	0.26 (0.24, 0.28)	6.2 (6.0, 6.5)	10.63 (10.20, 12.84)
	SLIP5	62.56	−173.55	66	15.3 (12.4, 18.8)	84.3 (81.2, 87.6)	1.2 (1.0, 1.3)	0.19 (0.17, 0.21)	6.1 (5.9, 6.4)	12.69 (10.86, 14.96)

Sediment grain size is reported as weight percent of sand (1–4 phi) and mud (≥5 phi); total organic carbon (TOC, mg g^{-1}); total organic nitrogen (TON, mg g^{-1}); carbon to nitrogen ratio of surface sediments (C/N); sediment community oxygen consumption (SCOC) rates (mmol O_2 m^{-2} d^{-1}; only reported from 2000 to 2012). Grain size, TOC, TON, C/N, and SCOC values are reported as medians and interquartile ranges (0.25, 0.75). Locations and water depths are average values for the five sites; see Table 1 for actual values. Data sources: Grebmeier and Cooper (2016*a*, 2018, 2019*b*, 2020).

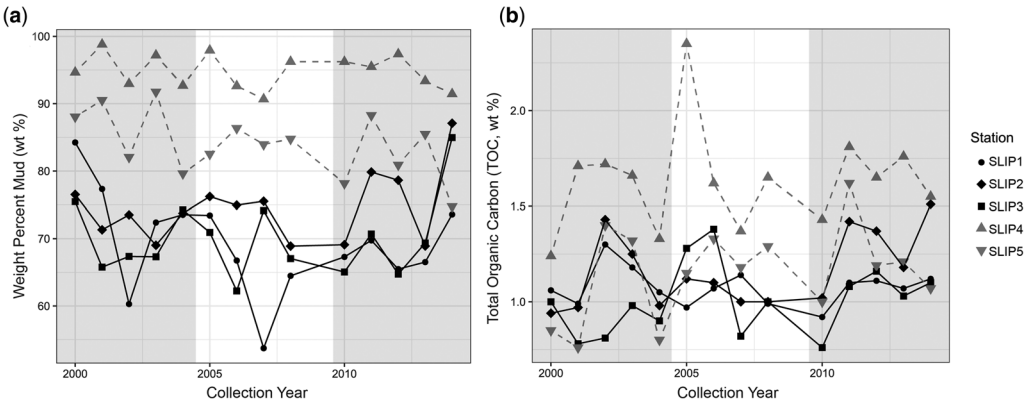

Fig. 2. Variation in (**a**) weight-percent mud (clay and silt, phi ≥ 5) and (**b**) total organic carbon (TOC, wt%) of the upper 0.5 cm of van Veen sediment grab samples at the same sample sites as the bivalve living and death assemblages. Alternating grey and white bands highlight the 5-year time binning of live data used in some analyses (2000–04, 2005–09, 2010–14; no data in 2009). Icon shapes denote different SLIP stations; solid black lines and icons used for sandy mud data (SLIP1–3), dashed grey lines and icons for mud (SLIP4–5) data from (Grebmeier and Cooper 2016*a*, 2018, 2019*b*). Mud content varied considerably year-to-year at each station, related to bottom current strength, with the sandy mud stations becoming muddier toward in 2014. TOC was similarly variable at all stations excepting SLIP4, where it was consistently higher.

on the 1 mm screen, compared to 3% remaining on the 0.5 mm screen; use of both screens produced more variable abundance levels due to the inclusion of meiofauna and juvenile macrofauna. Bivalve abundances were reported as living individuals per m^2 (indiv/m^2) of seafloor and reflect pooling of all replicate samples collected at a given station in each year, multiplied up to a standard 1 m^2. Acquiring 2–5 replicate samples per site per visit is standard among agencies, as is (among ecosystem scientists) the extrapolation of abundance data to a standard number per 1 m^2 (density). For analysis, these 'live data' were used both in their original annual form and after pooling into 5-year increments – 2000–04, 2005–09, and 2010–14 – to dampen noise and more closely simulate time-averaged data.

Bivalve dead-shell assemblages

Dead-shell assemblages were acquired from the same van Veen grab samples used to collect the living community in 2014, which was the last year of the time-series of live data used in this study. Such a single sampling of the dead-shell assemblage, coinciding with sampling the living community and extracted from the same sedimentary volume, is a standard procedure for live–dead comparisons (see review of protocols in Kidwell 2013). The sieve residue of shells, lithic gravel, and other debris was dried and sorted for mollusc shells at the University of Chicago. An empty, disarticulated bivalve shell or a shell fragment was counted as an individual if it retained ≥50% of the hinge line and was >1 mm in length and thus likely an adult. Still articulated, double-valved bivalve specimens were also counted as single individuals, but were rare: if these retained any flesh, they were removed and counted as living individuals. As with the live data, counts were multiplied to produce density values, i.e. the number of dead individuals per m^2.

We also acquired 'dead data' from van Veen samples collected in summer 2015, permitting a rare test of interannual variation in death assemblage composition. All live–dead comparisons (see methods below) were repeated using these 2015 death assemblages, which, unlike those collected in 2014, had potential to reflect individuals living in 2014. Results comparing live data and 2015 dead data were not significantly different than those comparing 2014 live and 2014 dead data, and so we report only the latter, which has been the conventional approach since the 1950s (Kidwell 2013).

Bivalve taxonomy and guilds

Each live and dead bivalve individual was identified to the lowest taxonomic level possible using print resources shared between the UMCES ARG and UChicago (Foster 1991; Coan *et al.* 2000). We also used two digital voucher collections: one created by the first author during visits to the ARG, and the other created by ARG collaborators to coordinate invertebrate researchers on the DBOs (Kędra and Oleszczuki 2017). With these resources, almost all bivalve specimens could be confidently

Table 3. *Taxonomic list and habitat-level occurrences of families, their guild (Todd 2001; Dufour 2005; Stead and Thompson 2006), and component species*

Guild	Family	Genus sp.	Sandy mud	Mud
Chemosymbiont	Thyasiridae		LD	LD
Chemosymbiont	Thyasiridae	*Thyasira flexuosa*		
Commensal	Lasaeidae		L	L
Commensal	Montacutidae		LD	LD
Commensal	Montacutidae	*Kurtiella* /*Mysella*/*Rochefortia tumida*		
Commensal	Montacutidae	*Kurtiella* /*Mysella planata*		
Commensal	Montacutidae	*Kurtiella* /*Mysella* sp.		
Epifaunal suspension	Mytilidae		LD	LD
Epifaunal suspension	Mytilidae	*Musculus discors*		
Epifaunal suspension	Mytilidae	*Musculus niger*		
Facultative deposit	Semelidae		L	L
Facultative deposit	Tellinidae		LD	LD
Facultative deposit	Tellinidae	*Macoma brota*		
Facultative deposit	Tellinidae	*Macoma calcarea*		
Facultative deposit	Tellinidae	*Macoma moesta*		
Facultative deposit	Tellinidae	*Macoma* sp.		
Facultative deposit	Tellinidae	*Macoma torelli*		
Infaunal suspension	Astartidae		LD	L
Infaunal suspension	Astartidae	*Astarte montagui*		
Infaunal suspension	Cardiidae		LD	LD
Infaunal suspension	Cardiidae	*Clinocardium ciliatum*		
Infaunal suspension	Cardiidae	*Clinocardium* sp.		
Infaunal suspension	Cardiidae	*Serripes groelandicus*		
Infaunal suspension	Cardiidae	*Serripes laperousii*		
Infaunal suspension	Carditidae		D	L
Infaunal suspension	Carditidae	*Cyclocardia* sp.		
Infaunal suspension	Lyonsiidae		L	
Infaunal suspension	Pandoridae		LD	
Infaunal suspension	Pandoridae	*Pandora* sp.		
Infaunal suspension	Thraciidae		L	L
Infaunal suspension	Ungulinidae		L	L
Infaunal suspension	Veneridae		LD	LD
Infaunal suspension	Veneridae	*Liocyma fluctuosa*		
Obligate deposit	Nuculanidae		LD	LD
Obligate deposit	Nuculanidae	*Nuculana radiata*		
Obligate deposit	Nuculanidae	*Nuculana* sp.		
Obligate deposit	Nuculidae		LD	LD
Obligate deposit	Nuculidae	*Ennucula tenuis* /*Nucula belloti*		
Obligate deposit	Yoldiidae		LD	LD
Obligate deposit	Yoldiidae	*Yoldia hyperborea*		
Obligate deposit	Yoldiidae	*Yoldia seminuda*		
Obligate deposit	Yoldiidae	*Yoldia* sp.		

Live-only ('L'), dead-only ('D'), or both alive and dead ('LD') occurrences in sandy mud (SLIP1–3) and mud (SLIP4–5) habitats. All taxa are infaunal unless otherwise noted.

identified to species level using shell morphology alone. The notable exceptions were many dead specimens of *Macoma*, which could typically be identified only to genus level owing to indistinctly preserved pallial lines or being represented only by hinge lines. Dead shells of commensal bivalves were also challenging. Given this challenge with the relatively abundant *Macoma*, and because most families in the fauna are represented by a single genus and usually a single species (Table 3), we used bivalve families as our unit of taxonomic analysis. This analytic coarsening of both live and dead data to the family level allows us to include all dead specimens, for a total of 17 families. All individuals from the bivalve families Lasaeidae and Montacutidae were treated as members of the superfamily Galeommatoidea because species and family-level assignments of living individuals in this superfamily have either been uncertain or changed over the 15 years of benthic sampling. Substituting this superfamily for the two separate families had no significant effect on the outcome

of our analyses, largely because of the rarity of both living and dead individuals. Overall, family-level identifications were earlier determined to suffice to differentiate living communities among all five DBO hotspots (Meadows *et al.* 2019) and they also suffice to differentiate among the five stations within the DBO1 hotspot analysed here.

Assignment of bivalve taxa to six guilds (Table 3) is based on a combination of life habit and trophic group, largely following Todd (2001): infaunal chemosymbiont-bearing, infaunal obligate deposit feeding (combines both surface and subsurface feeders), infaunal facultative deposit-feeding, infaunal suspension-feeding, epifaunal suspension-feeding, and commensals (live inside the body of another animal or share its burrow). Predatory bivalves (e.g. Cuspidariida), nestling (suspension-feeding) bivalves (e.g. Hiatellidae), and deep burrowing suspension feeding bivalves (e.g. Myidae) are not represented in the DBO1 fauna despite their presence in the Arctic region (likely gear-related undersampling of Myidae, although we also do not encounter dead shells of Myidae nor of the other taxa not occurring alive). For the purposes of these analyses, Yoldiidae were considered obligate deposit feeders (Stead and Thompson 2006) despite some evidence of flexible life habits (Todd 2001). Following Dufour (2005), the only facultative chemosymbiontic bivalve in this fauna is *Thyasira flexuosa*.

Live–dead comparisons

Live–dead comparisons used both raw (density, $\mathrm{indiv}/\mathrm{m}^2$) and proportional abundance data, and were conducted using both family- and guild-level resolution. Some comparisons here use annual-resolution data on the composition of living assemblages, but for most analyses we pooled annual data into five-year bins, both to reduce noise from interannual variation and to better approximate naturally time-averaged information. These temporal bins were 2000–04, 2005–09 (no live data for 2009), and 2010–14 (bins are shadowed in Fig. 2). Each year of live data, or each 5-year pooling of live data, was compared with data from the dead-shell assemblage collected in 2014. Pooling means that raw data were summed before any calculation (e.g. of proportional abundance) or data transformation. Spatially, all analyses were conducted at site-level resolution, but sites were informally grouped into a sandy mud habitat (sites SLIP1–3) and a mud habitat (SLIP4–5) for many figures, guided by the environmental information in Table 2.

To provide context for quantitative live–dead comparisons, we used bar graphs of the proportional abundance of guilds in the dead-shell (2014) and in each of the 5-year binned living assemblages. We also generated simple bivariate plots of living and dead-shell assemblages, using both raw density and proportional abundance of both guilds and families. Live–dead agreement was assessed using a Pearson correlation coefficient. Results (r-values) among these alternative plots were very similar, and so we only display plots of proportional abundance amplified by plots of the raw abundance of living individuals from the top four families over time.

For comparison with other systems, live–dead discordance was also assessed using a widely-used cross-plot of two measures of pairwise live–dead similarity: (1) in the rank abundances of taxa, expressed as a correlation (Spearman's rho), and (2) in the presence–absence of taxa, i.e. the proportion of taxa shared by two lists after correction for disparate sample sizes, Jaccard–Chao index (JC), following Kidwell (2007). A positive Spearman ρ indicates that taxa that numerically dominate the living assemblage are also highly ranked in the death assemblages and that taxa that are rare in one assemblage are also rare (or absent) in the other; a ρ of 1 denotes that taxa are ranked identically in both assemblages. JC uses information on the numbers of singletons and doubletons to correct for 'unseen taxa' in the smaller sample (Chao *et al.* 2005); a JC of 1 indicates that the lists of live and dead taxa are identical, with all species shared and none occurring dead-only or live-only. Here, both JC and ρ are calculated using bivalve families. When displayed on a cross-plot, stations falling in the upper-right quadrant have the least live–dead discordance. This method has previously only been used with numerical abundance data for *species*, and originally only at the *habitat level*, i.e. after data from multiple stations within sedimentary facies had been pooled (Kidwell 2007). Here, discordance is evaluated using numerical abundance of *families* at the *station level*, and for every pairwise comparison of annual live data (2000–14) with dead data collected in 2014.

Nonmetric multidimensional scaling (NMDS) has also become widely used in live–dead analysis to recognize compositional differences in multivariate space. It differs from other unconstrained ordination methods by representing multidimensional data in a low number of predetermined axes, and approaches that solution through an algorithmic approach rather than through eigen-decomposition in order to minimize rather than maximize pairwise distances between sites (Borcard *et al.* 2011). We used wisconsin-transformed abundance data from the three sets of five-year binned live data and from the once-sampled dead data. All NMDS spaces were constructed using extended Jaccard distances, closely related to the Bray–Curtis dissimilarity (B, where the extended Jaccard $= 2B/(1 + B)$; Oksanen *et al.* 2007). Semelidae and Pandoridae were excluded from these family-level analyses because of low singleton abundances, both living and dead.

Guild-level data were not tested because the low number of overall guilds did not yield a converged solution with low stress in NMDS. A NMDS with low stress (e.g. <0.1) maintains differences between sites while limiting distortion of the original distance matrix.

All data analyses were performed using R and the vegan (Oksanen *et al.* 2007), stats (R Core Team and Contributors Worldwide 2022), fossil (Vavrek 2020), and trend (Pohlert 2020) packages, and all visualizations and plots were created using ggplot2 (Wickham *et al.* 2022).

Results

Qualitative spatial and temporal variation in abundance

Bar graphs of the proportional abundance of guilds and families show that bivalve death assemblages from each within habitat (sandy mud SLIP1–3, and mud SLIP4–5) resemble each other more closely than they resemble death assemblages from the other habitat (Fig. 3, left column). At sandy mud sites, obligate deposit feeders dominate overwhelmingly (90–95% of all dead individuals), and Nuculanidae dominates that guild overwhelmingly. At mud sites, obligate deposit feeders also dominate the dead but less strongly (65 to 78%); Nuculanidae dominates that guild here, too, as in sandy mud, but less strongly. In both habitats, facultative deposit feeders constitute the remainder of the death assemblage, mostly *Macoma* (Tellinidae), with scarce specimens of other guilds and families.

Living assemblages also differ between the two habitats (Fig. 3 right three columns, Figs 4 & 5). At sandy mud sites, compositions decreased monotonically from an overwhelming dominance by obligate deposit feeders in 2000–04 (80–89%) to $<50\%$ by 2010–14, when the facultative deposit feeding Tellinidae attained dominance (Fig. 3, upper two rows); exceptionally, epifaunal suspension feeding Mytilidae were coequal with Tellinidae at SLIP2 in 2010–14. Within the obligate deposit-feeding guild, families shifted strongly in relative importance, with dominance shifting progressively from Nuculanidae to Nuculidae, and with Yoldiidae at SLIP3 comprising up to 14% of individuals in 2005–09. In contrast, at mud stations, obligate deposit feeders were the dominant guild in living assemblages over the entire 15-year monitoring series. At SLIP4, Nuculanidae and Nuculidae remained co-dominant, with substantive Yoldiidae in 2000–04, whereas at SLIP5, Nuculidae progressively rose to a clear dominance with negligible appearance of Yoldiidae (Fig. 3, lower two rows).

Inspection of these bar graphs also shows that live–dead agreement is generally highest when death assemblages are compared to the oldest sampling of the live, both at the family-level and especially considering guild-level composition (Fig. 3). In mud stations, live–dead agreement at the guild level is high for all live samplings because the guild composition of the living communities was relatively consistent throughout the time-series despite changes in the proportions of families (Fig. 3, bottom two rows, all columns). At the family level, the 2014-collected death assemblages at all stations are enriched in Nuculanidae compared to every sampling of the living, but most closely resemble the oldest (2000–04) live collections (except at SLIP4) and differ most strongly from the most-recently sampled living assemblage (2010–14, including at SLIP4).

Interannually, the total abundance of bivalves per station ranged from 130 to 2673 indiv/m^2 (median 679 indiv/m^2; grey icons and dashed lines in Figs 4 & 5). Living bivalve abundance was several times larger in mud stations than in sandy mud stations (median 1327 indiv/m^2 v. 527 indiv/m^2, respectively). At sandy mud stations, total abundance peaked in 2005–08, and then declined to its lowest level in the time-series in 2011; bivalve abundance recovered to earlier levels by 2012–14 (Fig. 4a; not evident in Fig. 5a due to temporal binning), coincident with a slight increase in the percent mud in the seabed (Fig. 2a). At mud stations, total bivalve abundance showed less strong changes interannually and less coordination between the two stations (dashed lines in Fig. 4b), but each station showed a several-fold change over the 15-year time-series: total abundance increased at SLIP4 and decreased at SLIP5 (dashed lines in Fig. 5b).

Family abundances at sandy mud stations were highly variable interannually (Fig. 4a) but, overall, the facultative-deposit feeding Tellinidae increased steadily in absolute numbers at all stations by several-fold, and the obligate deposit-feeding Nuculanidae declined by an order of magnitude over the same period (Fig. 5a). Other obligate deposit-feeding families in sandy mud exhibited a broad increase followed by a decrease, with either no net change or a slightly lower abundance at the end of the time-series than at the start (Fig. 5a). Interannual resolution reveals strong swings in abundance in all families (Fig. 4a, note order of magnitude changes in family abundance). Yoldiidae, for example, increased to several hundred indiv/m^2 in 2005–07 before declining back to $\leq$10 indiv/m^2.

Family abundances at mud stations are less temporally variable than in sandy muds using both interannual (Fig. 4b) and time-binned data (Fig. 5b). Total bivalve abundance rose steadily at SLIP4 and declined steadily at SLIP5, correlating respectively with a strong increase and strong decrease in the raw abundance of Nuculanidae (Fig. 5b). Other families followed the trend of Nuculanidae, with the

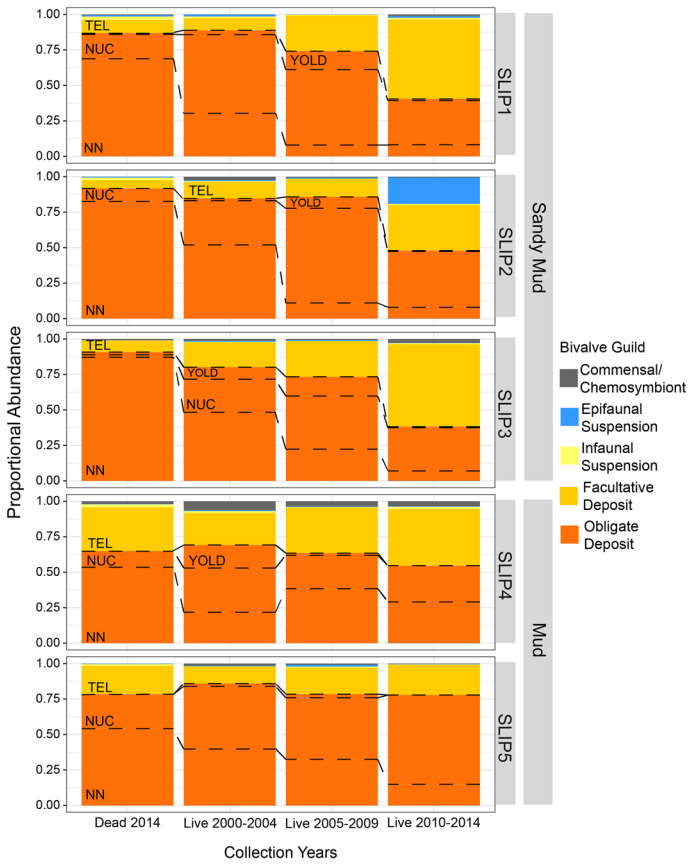

Fig. 3. Proportional abundance of bivalve guilds in the dead-shell assemblage (left column) and in successive living assemblages at each of the DBO1 stations (SLIP1–5), with live data pooled into 5-year bins. The dominant guild of infaunal obligate deposit feeders is subdivided into families (NN, Nuculanidae; NUC, Nuculidae; YOLD, Yoldiidae); the infaunal facultative deposit-feeding guild comprises a single family (TEL, Tellinidae). Stations are grouped by habitat (facies). Obligate deposit feeders dominate the death assemblages at all five sites, and also dominate the oldest living assemblages everywhere, but decline in proportional abundance over the live time-series (except at SLIP5), accompanied by a shift in the family composition of that guild. Nuculanidae are far less abundance in the youngest living assemblage than in the death assemblage everywhere, and in the sandy mud sites, the facultative deposit-feeding Tellindae are proportionally far more abundant living than dead.

exception of Yoldiidae, which declined strongly at both stations by two orders of magnitude (from $\geq$100 indiv/m^2 to only a few, also evident in time-binned data Fig. 5b). In interannual data (Fig. 4b), almost all families at both mud stations exhibited a local peak within the 2005–08 interval, as also observed in sandy mud stations (Fig. 4a).

Quantitative live–dead comparisons

Live–dead agreement in the proportional abundances of guilds and of families are compared directly in Figures 6 and 7, with agreement expressed by their Pearson correlation (r, upper left corner of each live–dead cross-plot, 5-year binning of live data). Live–dead agreement is positive for both guild- and family-level data in all comparisons but varies with data resolution (higher r using guild-level data; Figs 6 & 8a), and over time (decreasing as the dead data are compared with more recently collected living assemblages, except at SLIP4; Fig. 8). Using guild-level data (Fig. 8a), live–dead agreement is very high ($r >$0.95) for early samplings of the living assemblage in both habitats, but it declines markedly in sandy mud stations with the most recent sampling (2010–14; to $r = 0.8$ at SLIP2 and to $r =$ 0.5–0.6 at SLIP2–3). In mud stations, live–dead agreement remains high throughout the time-series at $r >$0.95 (Fig. 8a). Using family-level data (Figs 7 & 8b), live–dead agreement in the sandy mud stations starts

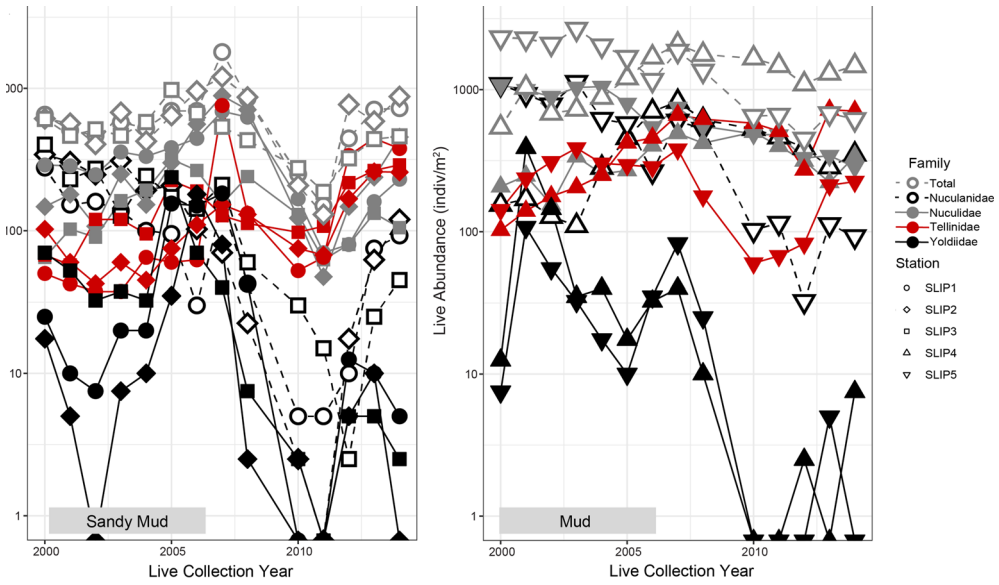

. **4.** Annually sampled abundance (standardized to number of individuals per m^2) by station of all living bivalves ıl; icons with grey outline) and of the four dominant families by station from 2000 to 2014, showing the highly able density data behind the temporally-coarser shifts in proportional abundance displayed in Figure 3. (**a**) ions from sandy mud seabeds at SLIP1, 2, and 3; (**b**) stations from mud seabeds at SLIP4 and 5 (Grebmeier and ɔper 2016*a*, 2019*a*, *b*).

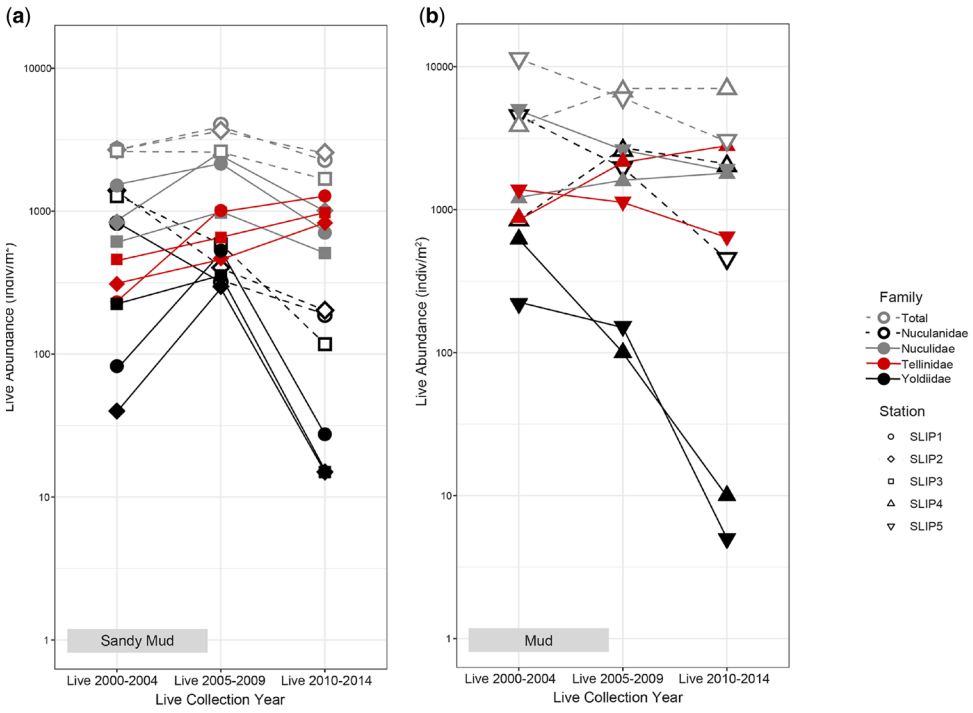

. **5.** Abundance (indiv/m^2) of the total bivalve living assemblages and their dominant families at each station after ling data into 5-year bins: (**a**) sandy mud habitats (SLIP1–3); (**b**) mud habitat (SLIP4–5).

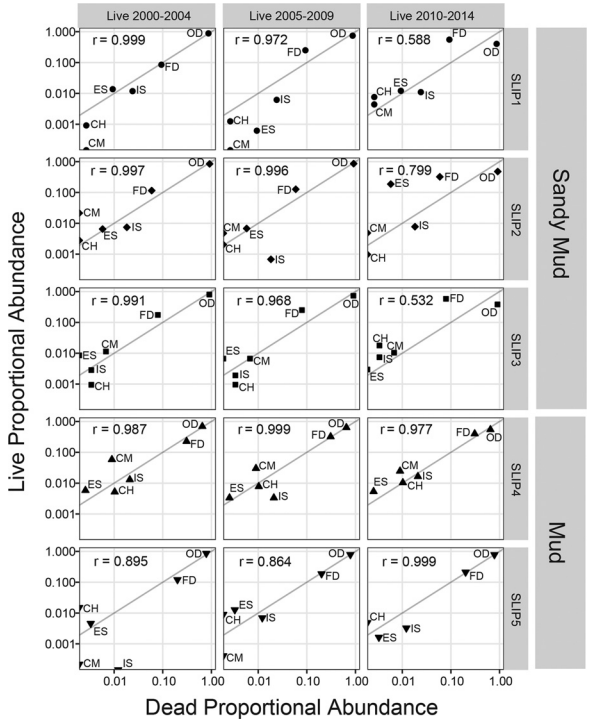

Fig. 6. Bivariate plots of the proportional abundance of bivalve guilds in living and death assemblages by station; death assemblages collected in 2014, live data reflect pooling of annual samples into 5-year bins. Data points that fall on the *x*- or *y*-axis indicate that the guild occurred dead-only or live-only, respectively. Note log-scales of axes, for display only. Diagonal grey line denotes a 1:1 relationship, i.e. perfect live–dead agreement; *r* is the Pearson coefficient of correlation of data points. Guild labels: OD, obligate deposit feeder; FD, facultative deposit feeder; ES, epifaunal suspension feeder; IS, infaunal suspension feeder; CH, chemosymbotic, CM, commensal.

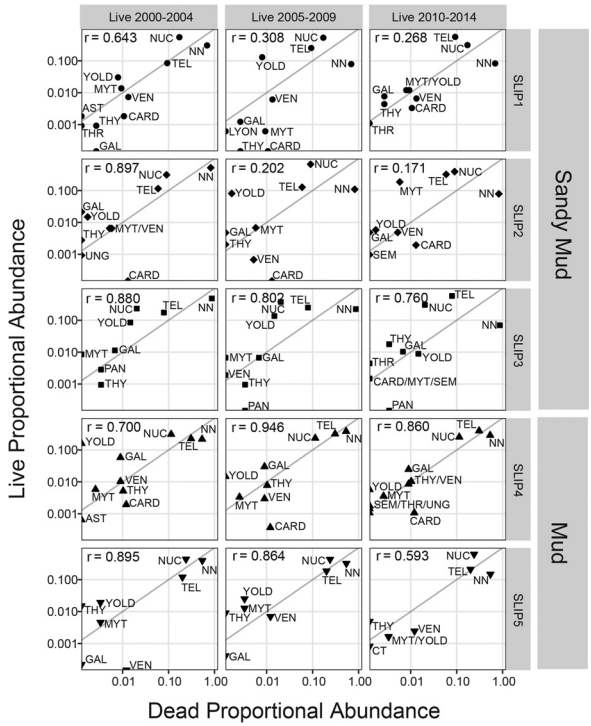

Fig. 7. Bivariate plots as in Figure 6 but using the proportional abundance of bivalve families. Family labels: NUC, Nuculidae; NN, Nuculanidae; CARD, Cardiidae; TEL, Tellinidae; YOLD, Yoldiidae; MYT, Mytilidae; VEN, Veneridae; THY, Thyasiridae; GAL, Galeommatoidea; THR, Thraciidae; UNG, Ungulinidae; AST, Astartidae; SEM, Semelidae; PAN, Pandoridae; and CT, Carditidae.

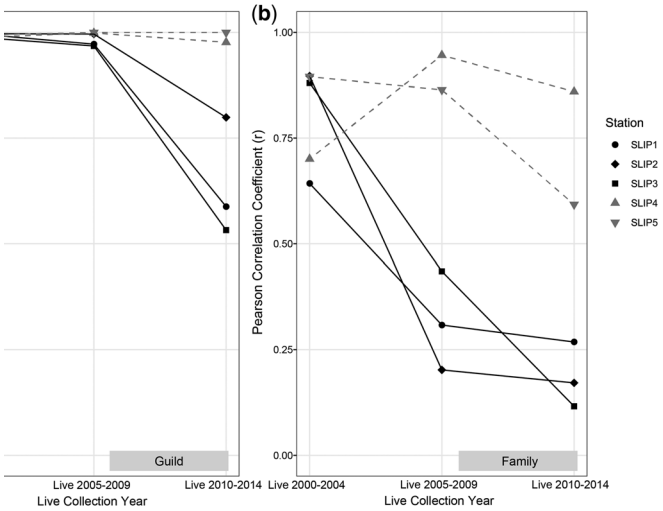

ad agreement (Pearson correlation) as the death assemblage (from 2014) is compared to sampled living assemblages, by station. (**a**) Using guild-level data (Pearson *r* values from el data (Pearson *r* values from Fig. 7). Stations SLIP1–3 are from sandy mud seabeds ols), SLIP4–5 are from mud seabeds (dashed grey lines and symbols).

ıd declines steadily, again n the most recent sampling l stations, live–dead agree- nes from a high value the most recent sampling, LIP4, agreement increases slightly toward the most recent sampling from r ~0.7 to ~0.85. Live–dead agreement in the mud stations is never as low as in the sandy mud stations, using either guild- or family-level data (Fig. 8).

With few exceptions, cross-plots of the live–dead rank-abundance correlation of taxa (Spearman's ρ)

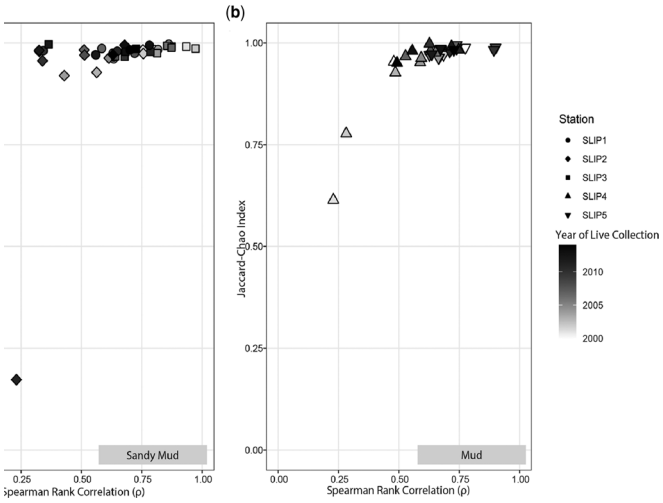

nt at the family-level evaluated using a cross-plot of taxonomic similarity (shared taxa, and dead sample sizes; Jaccard–Chao index) and the rank-order agreement in family nan ρ). Each symbol represents live–dead agreement at a single station for the living articular year, shaded by year of collection (dark colours = earlier collections); each assemblage collected in 2014. Perfect live–dead agreement would fall at the upper right ons from sandy mud seabeds; (**b**) results for stations from mud seabeds. All Spearman nd thus plots are truncated for easier viewing of data.

against live–dead taxonomic similarity (JC index) reveal overall very high agreement in family composition in both sandy mud and mud habitats (Fig. 9). With few exceptions, $\rho \geq 0.5$ and JC ≥ 0.85. Each icon reflects comparison of the living assemblage sampled in a given year between 2000 and 2014 against the death assemblage collected at that same site in 2014; variation in live–dead agreement per site thus arises from interannual variability in the living assemblage.

At sandy mud sites (SLIP1–3; Fig. 9a), live–dead agreement varies interannually most strongly in rank-abundance (ρ), with consistently very high taxonomic similarity (JC $\geq$0.91); the one exception (with JC = 0.17) is a very small live sample from 2011. The sample-series from SLIP1 has one outlier of relatively low ρ (live sampled in 2010, ρ *c.* 0.3), but otherwise ranges narrowly between $\rho = 0.55$ and 0.77 (Fig. 9a), and the SLIP3 series is similar (one low-ρ outlier from 2012 at 0.36, otherwise $\rho = 0.6$–0.95; Fig. 9a). SLIP2 shows the greatest interannual variation in live–dead agreement, with on average lower ρ (0.3 to 0.75); the lowest ρ values are from 2006, 2011, and 2012.

In the two mud sites (SLIP4–5; Fig. 9b), live–dead agreement is consistently high at SLIP5, signaling that the relative abundances of families in the living assemblage are both quite consistent over time and similar to that of the death assemblage (as also seen in Fig. 3): ρ varies only between 0.63 and 0.90, and JC is always $\geq$0.96. SLIP4 exhibits the greatest variability in live–dead agreement of all five sites, with ρ varying from 0.23 to 0.75 and JC ranging down to 0.62 from a maximum of 1.00. The poorest live–dead agreement is found when the SLIP4 death assemblage is compared with living assemblages

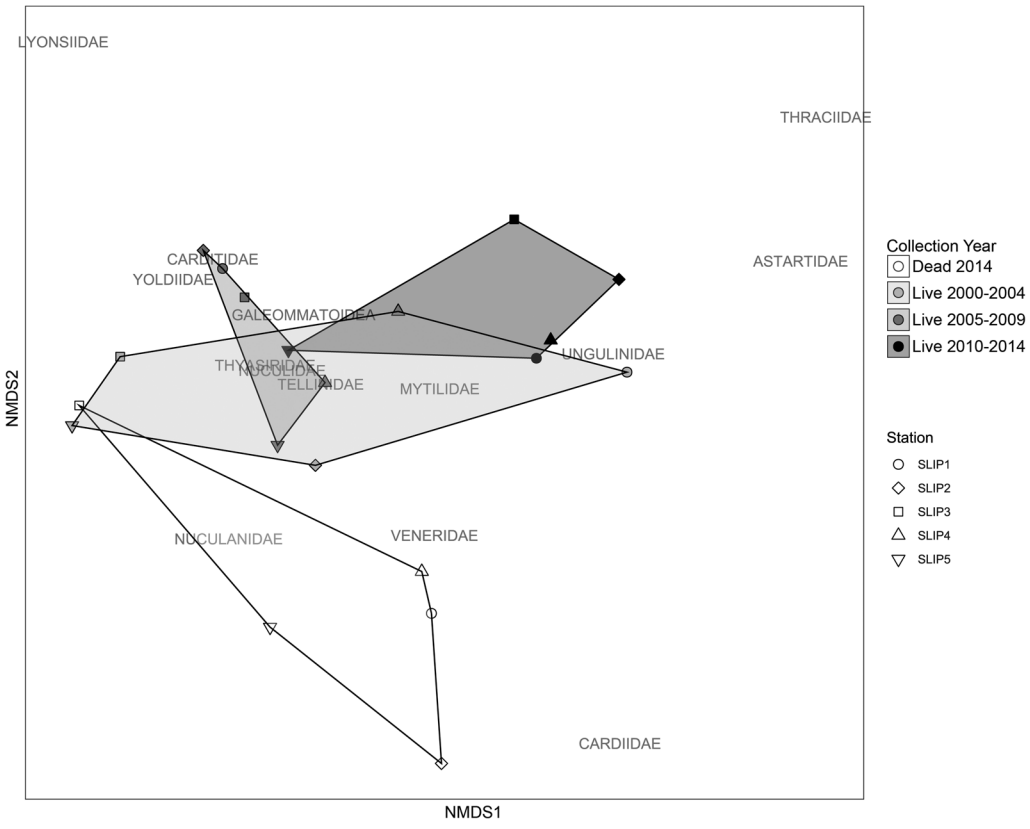

Fig. 10. Multivariate comparison of living assemblages (5-year binned data) and death assemblages from the entire DBO1, using nonmetric multi-dimensional scaling (NMDS); each assemblage is hulled to ease viewing, showing only the first two axes. NMDS was constructed using family-level abundance data, scaled using the square-root Wisconsin transformation, extended Jaccard distance, $k = 3$, stress = 0.107, tries = 20. Death assemblages lie apart from all living assemblages, excepting SLIP3, related to higher abundances of the obligate deposit-feeder Nuculanidae and subsidiary Veneridae and Cardiidae (infaunal suspension feeders); all death assemblages are compositionally furthest from living assemblages collected most recently (2010–14).

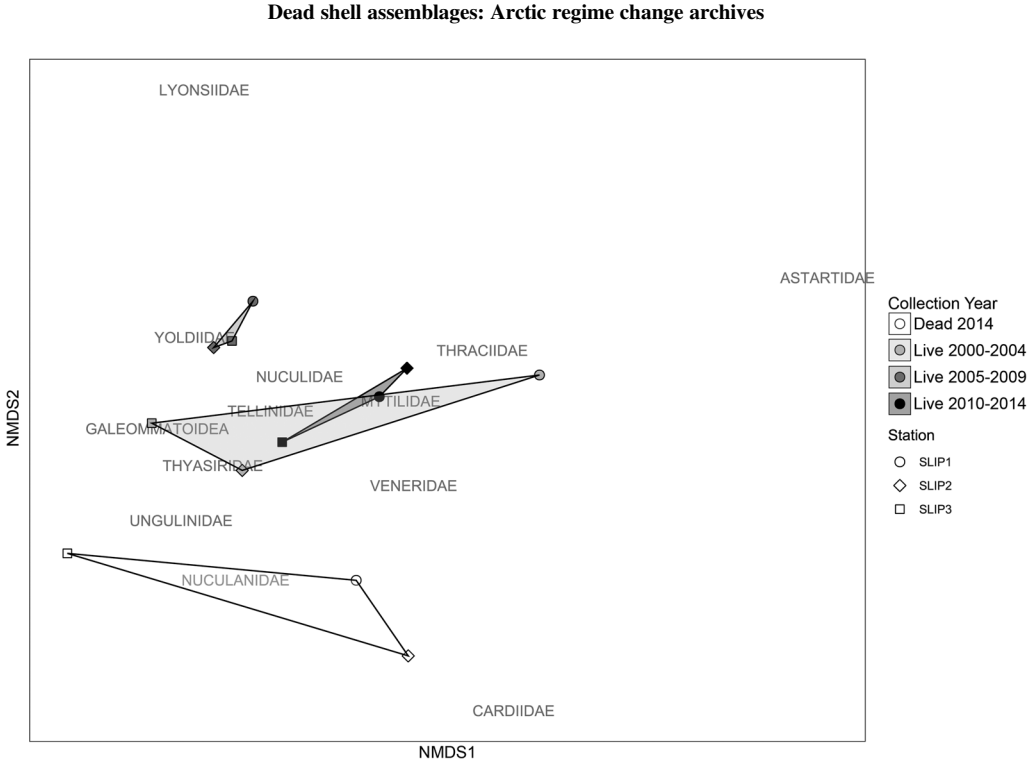

Fig. 11. As Figure 10, but with NMDS axes calculated using only the three sandy mud stations (SLIP1, 2, 3). Stress = 0.020, tries = 20.

from the earliest part of the live time-series (lowest agreement in 2001, followed by 2002, followed by 2000), despite reasonable sample sizes ($n = 1035$, 542, 680 living individuals per m^2, respectively, compared with 3839 dead individuals per m^2).

In general, using JC–ρ cross-plots (Fig. 9), live data collected early in the 15-year time-series resembles the death assemblage most closely, but the correlation of agreement with collection year is not consistent because live variability is especially high at all sites in the 2005–10 interval, as also evident in Figure 4.

Multivariate analysis (NMDS) using family-level data pooled into 5-year bins (Fig. 10) shows that death assemblages differ in composition from all source living assemblages, specifically in having more obligate deposit-feeding Nuculanidae and infaunal suspension-feeding Veneridae and Cardiidae (with the exception of sandy mud site SLIP3, whose death assemblage most closely resembles its 2000–04 living assemblage). The most-recently collected living assemblages (from 2010–14) are furthest from their counterpart death assemblages at all sites, whereas living assemblages from the earliest and middle phases of the live time-series overlap with each other and are closest to the death assemblages. Yoldiidae and infaunal suspension-feeding Carditidae (*Cyclocardia*) are important in the middle phase of the live time-series, especially at the three sandy mud sites (as also evident in Fig. 3). In general, the living assemblages are characterized by larger proportions of Tellinidae, epifaunal suspension-feeding Mytilidae, and infaunal suspension feeders other than those already listed.

Considering only the three sandy mud sites (Fig. 11), death assemblages plot closest to each other and "near" Nuculanidae along axis 2; they do not overlap with any of the living assemblages, but are closest to the oldest living samples (2000–04) and are furthest from the mid-series samples (2005–10). Living assemblages contain larger numbers of other families of obligate deposit feeders, of facultative feeders, and of all infaunal suspension feeders other than Cardiidae. Considering only the two mud sites (Fig. 12), death assemblages (white-filled icons) lie among the three successively sampled living assemblages.

Discussion

For death assemblages to serve as reliable archives of community ecology over the recent past, their composition must not have been overtly biased by taphonomic processes, notwithstanding time-averaged accumulation in the surface mixed layer. Preferably,

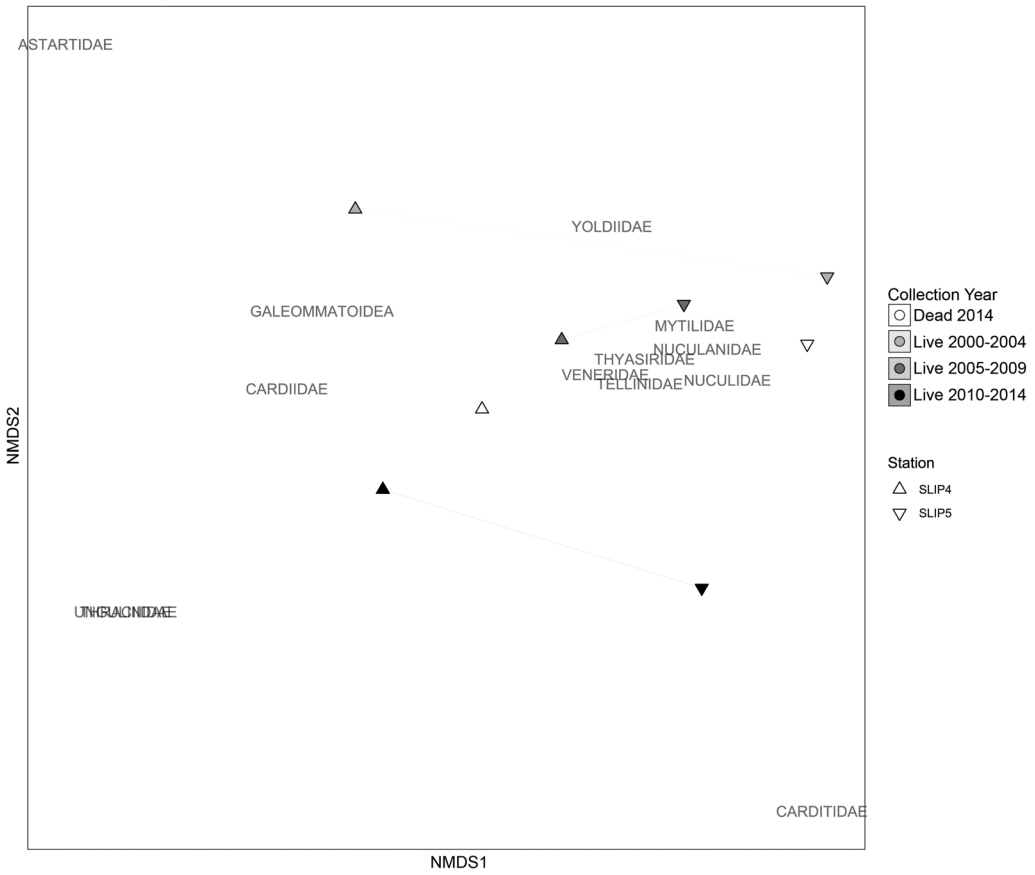

Fig. 12. As Figure 10, but with NMDS axes calculated using only the two mud stations (SLIP4 and 5). Stress = 0.020, tries = 20.

live–dead differences in composition reflect ecological changes during the interval of time-averaged accumulation, and do not arise from differential preservation of species. These and other possible causes of live–dead discordance can be treated as a series of hypotheses (H1–5) that can be evaluated in turn but are not mutually exclusive (Table 4; adapted from Kidwell 2013).

Hypothesis 1: live–dead differences arise from shortcomings of method and sampling

These issues were likely negligible in this study of DBO1. Living and dead-shell assemblages were sampled using the same van Veen grab and 1 mm processing, with the death assemblage sieved from the same set of samples used to acquire living assemblages in 2014. Favouring sufficient sample sizes, the ratio of dead:live individuals in DBO1 was on average 6:1, notably higher than the *c.* 1:1 ratio encountered in other DBOs of the Bering–Chukchi seas (Meadows *et al.* 2019) and other boreal and cold-temperate seabeds (Kidwell 2013). This ratio is comparable to the median 8:1 dead:live ratio encountered in warm temperate and tropical shelves, where small *live* samples are the most common challenge. Dead samples in the highly productive DBO1 were thus sufficiently large to ensure confident proportional abundance data (>4500 dead bivalve indiv/m^2 compared to a median 679 live bivalve indiv/m^2). Exceptionally, the density of four annual live samples were <250 indiv/m^2, which in raw terms meant an average of only 15 bivalve individuals per 0.1 m^2 grab. Such low numbers in the 2011 sampling of the living assemblage at SLIP2 produced exceptionally low JC and ρ values in Figure 9a. However, none of the other four samples with a live n <250 indiv/m^2 displayed this effect, and the 5-year binning of annual samples counteracted these sparse samples in other analyses.

Table 4. *Protocol for evaluating the underlying causes of strong live–dead discordance in the relative abundance of a taxon or set of taxa in benthic samples from the surface mixed layer*

Hypothesis	Explanation for observed live–dead discordance
H1: Shortcomings of method, sample size or quality issues	Small number of living or of dead individuals per sample or in the total number of samples for any reason, including taxa that are difficult to collect alive using available gear, post-collection damage of sample, operator errors in identification or counting; *dead sampled using different methods than live samples*
H2: Contamination or culling of death assemblage	Death assemblage altered by human activities, e.g. beach replenishment, dredge spoil dumping, shell removal (shell-fishery, -trade, -mining)
H3: Time-averaging	Death assemblage reflects input over time, compared to a 'snapshot' of the living community; *all naturally occurring dead-shell assemblages are assumed to be time-averaged to some extent, typically on the order of decades to centuries, which can be quantified by geological age-dating*
H4: Taphonomic bias	Death assemblage composition altered by natural postmortem processes, i.e. acting upon inter-species differences in shell production, durability, and/or transportation. *Includes biasing effects of preferential predation (and thus removal) of individuals of a particular taxon or body-size class*
H5: Ecological change	Living assemblage changed during the window of time-averaging in response to natural or anthropogenic factors, (e.g. change in taxon presence–absence, proportional abundance, production rate, density, inherent durability), *or change in the intensity of shell removal related to the ecological change, (*e.g. *predation, oxygenation)*; death assemblage remembers the former community state

Hypotheses (H) are not mutually exclusive. Adapted from (Kidwell and Tomašových 2013); italics denote addition here.

The same set of voucher specimens were used for taxonomic identification of both datasets, ensuring consistency. We further minimized live–dead differences arising from H1 by coarsening all identifications to the family level given the difficulty of differentiating (abundant) dead specimens of Tellinidae to species level. We coarsened data for the commensal taxa *Mysella*, *Rochefortia*, and *Kurtiella* to superfamily level given unstable family-level assignments.

Van Veen grab samples are well known to undersample living individuals of large-bodied bivalves and especially individuals living deeper than 20–30 cm below the sediment–water interface, which here would include deep-burrowing Myidae and some commensal Galeommatoidea. Dead shells of deep-dwelling animals might be reworked upward, i.e. within the reach of a van Veen grab, and so gear bias might in principle be stronger against living than dead individuals. However, in our study, the numbers of individuals of deep burrower groups tended to be very low both alive and dead. The effect of missing large individuals (especially Myidae) is further diminished here by using numerical abundance rather than biomass as the currency of analysis; most bivalve individuals would live within the depth of penetration of the gear. Commensal galeommatoids, which can live inside other animals or share their burrow, often elude detection as living individuals, are commonly assigned to species inconsistently, and their dead shells can be extremely difficult to differentiate, even at the family level (many are edentate and identified with soft tissue characteristics). As a result, we ran our analyses both including and excluding commensal individuals and found no effect, even though they were abundant alive at SLIP4 in the 2000s.

We thus conclude that methodological and sample-size issues (H1) make a negligible contribution to observed live–dead discordance in DBO1.

H2: contamination or culling of death assemblage

We have no reason to suspect any human activities that would have either introduced or selectively removed dead bivalve shells at these sites. Bottom-trawling, for example, has been restricted to the southern Bering Sea since the early twentieth century by the United States and was reaffirmed in 2009 to further protect untrawled seas (NOAA 2008; NOAA NMFS 2012). All removal and/or transport of shells within DBO1 is likely natural, for example from the locally intense activity of benthic-feeding spectacled eider ducks (*Somatera fuscgeri*) and

Pacific walrus (*Odobenus rosmarus divergens;* discussed in H4).

H3: time-averaging of shell input

Death assemblages in the northern Bering Sea are assumed to be time-averaged to some degree given well-oxygenated overlying waters (thus ample bioturbation, which will mix young shells downward and older shells upward), abundant shelled infaunal animals (thus positive shell input), and moderate rather than rapid rates of sedimentation (thus slow net burial; here 0.1–0.5 cm a^{-1}; Cooper and Grebmeier 2018), all typical conditions for siliciclastic continental shelves. Given time-averaging, some offsets in composition are to be expected, even in the absence of taphonomic bias. For example, in meta-analyses, live–dead agreement in 'pristine' settings can range from 1 down to 0.5 using presence–absence measures of taxonomic similarity (JC), and from 1 down to 0.5 using Spearman rank-order correlations, simply from natural levels of variability (Kidwell 2007). The composition of the time-averaged death assemblage will also tend to diverge from any single instantaneous sample of the living, owing simply to the difference in temporal resolution of the dead and living samples, and both the richness and evenness of the death assemblage will be higher, due to the summing of short-term variability in the system (effects summarized in Kidwell and Tomašových 2013). Under steady-state conditions, modelling reveals that the composition of an accumulating death assemblage converges quickly toward the average composition of living assemblages within the first five to ten years of time-averaging, summing across short-term changes in dominance and capturing ephemeral rare taxa (Tomašových and Kidwell 2011).

With few exceptions, annual-resolution live–dead agreement here is consistently high using Spearman rank-order correlations ($\rho \geq 0.5$) and using presence–absence-based measures of taxonomic similarity (JC >0.85), except with comparisons from the end of the live time-series (Fig. 9). Therefore, time-averaging (H3) might suffice to explain compositional offsets up until shifts near the end of the living time-series. Pooling of live data into five-year bins for the NMDS analyses should, on the one hand, diminish live–dead compositional offset – the temporally pooled live data should mimic time-averaging – but on the other hand the use of proportional abundances represents a more sensitive test than those using only rank abundance or presence–absence. In sandy mud sites (SLIP1–3; Fig. 11), death assemblages are consistently distinct from any of the living assemblages, falling outside the range of compositions observed at any time. Thus, some factor(s) other than H3 must be responsible for the clear live–dead offsets in composition based on proportional abundance. In contrast, death assemblages from mud sites (SLIP4–5; Fig. 12) fall along the periphery of the multivariate cloud of points produced by live samples, a result that is more consistent with time-averaging (H3) as an important if not dominant process. Thus, time-averaging suffices to explain most live–dead differences in the mud sites but does not suffice in the sandy mud sites that lie closest to the fluctuating cold bottom water pool and ice edge (Figs 1 & 10–12), nor does it suffice in either habitat to explain live–dead discordances using living assemblages from the end of the time-series (Fig. 9).

Our preliminary age-dating of bivalve shells from DBO1 seabeds using ^{14}C-calibrated amino-acid racemization indicates that the magnitude of time-averaging in these cold, bioturbated, organic-rich seabeds is shorter than that documented in warm-temperate and tropical shelf seabeds (Meadows 2020; Meadows *et al.* 2020). In DBO1, using data from *Nuculana* and *Macoma*, median shell ages are 50 years, interquartile ranges (IQRs) are $<$100 years, and the oldest dated shell is 400–1200 years (74 total dates). These values contrast with median ages of 500–1000, IQRs of 1000–2000 years, and shell ages up to 20,000 years in warm temperate and tropical shelves (Krause *et al.* 2010; Kidwell and Tomašových 2013; Tomašových *et al.* 2014, 2018). The relatively narrow window of time-averaging in these Bering Sea bivalve death assemblages would diminish the live–dead contrast in temporal resolution and thus tend to diminish the magnitude of effect expected from H3 on live–dead contrast in species composition. Such a short window of time-averaging means that these Arctic dead-shell assemblages provide a relatively high-resolution source of information for ecological analysis, with negligible memory beyond the most recent few centuries of ecological history and a strong memory of only the most recent century. Additional dating and calibration effort are underway to confirm these initial estimates.

H4: Taphonomic bias

Skewing of death assemblage composition away from that of the local, source living assemblages, owing to interspecies differences in shell durability (affecting rate of loss), production (i.e. differences in rate of shell input related to lifespans and fecundity), and transport (causing either loss or input of shells), has potential to be a significant factor in these seabeds, which we suspected would be especially corrosive to bivalve aragonite (see 'Study area'). Both facies are from the middle shelf (66–82 m; Tables 1 & 2) between fair-weather and storm wave bases, evident from their mix of mud

and sand, with consistently well-oxygenated overlying water that supports intense bioturbation. Physical currents on this low-gradient middle shelf are thus unlikely to cause significant, i.e. spatially-homogenizing, preferential transport of shells and shell fragments >1 mm, either into or away from the life habitat, based on studies of other low-gradient shelves (Flessa 1998; Kidwell 2008; Tomašových and Kidwell 2009; Weber and Zuschin 2013; Albano *et al.* 2018; Gilad *et al.* 2018). Storms typically fail to homogenize the composition of dead-shell assemblages even in much shallower level-bottom settings (Hassan 2015; Casebolt and Kowalewski 2018; Brown and Larina 2019). We thus focus on other taphonomic agents.

A priori, the higher TOC and sediment oxygen consumption at the mud sites (SLIP4–5; Table 2) could generate particularly unfavourable porewater conditions for aragonite persistence, with these conditions producing more acid by biological irrigation and potentially promoting faster microbial decomposition of shell microstructures (Aller 1982; Emerson *et al.* 1990). However, TOC and, most importantly, benthic respiration are fairly high at all sites throughout DBO1 and so we do not expect particularly strong facies-level variation in shell preservation (Table 2). In addition, seasonally strong aragonite undersaturation of the overlying water was experienced throughout the northern Bering Sea during our study period; although correlated with benthic productivity, undersaturation is not solely localized to the highest productivity sites within the northern Bering Sea (Mathis *et al.* 2011, 2014; Cross *et al.* 2018). Finally, shell durability also presents little leverage for differential preservation of taxa within sites, because the bivalve fauna of DBO1 is entirely aragonitic with the exception of bimineralic Mytilidae, which occur only sporadically.

We thus look instead to interspecies differences in maximum body size, shell thickness, and microstructure that might affect durability, but again conclude that these probably had little net effect on death assemblage composition. For example, the live time-series (Figs 3–5) reveals an absolute and proportional increase in Tellinidae, especially in the muddy SLIP4–5 sites. Many Tellinidae are typically relatively thin-shelled, with lower inherent preservation potential than thicker shelled Veneridae, Astartidae, and Carditidae, which are also present in DBO1 communities. In southern California shelf death assemblages, for example, small-bodied, thin-shelled species of *Tellina* are disproportionately rare compared to their known population history (Leonard-Pingel *et al.* 2019). However, in DBO1, Tellinidae is represented by relatively large-bodied, comparatively thick-shelled species of *Macoma*, and so we suspect that their lower abundance dead than alive is not taphonomic in origin.

In contrast, the shells of Lyonsiidae, Pandoriidae, and Yoldiidae here and elsewhere are all extremely thin and composed of high-organic aragonitic microstructures prone to rapid disintegration (Glover and Kidwell 1993; Harper 2000; Valentine *et al.* 2006). These families do in fact consistently occur more abundant alive than dead in DBO1, consistent with taphonomic under-representation (Fig. 10). These taxa are also, however, scarce (<1%) even in the few living assemblages where they occur (e.g. SLIP3), and so their under-representation in death assemblages has negligible effect on live–dead discordance.

Finally, the shells of Nuculanidae and Nuculidae, although relatively thick for their size, should have relatively low inherent preservation potential in most settings arising from their high-organic nacreous and homogeneous aragonitic microstructures. Their disproportionately high abundance in all DBO1 death assemblages (e.g. Fig. 3) is thus contrary to taphonomic bias, which should make them disproportionately rare. Consequently, although preservational bias arising from interspecies differences in shell durability probably contributes to observed live–dead discordance to some degree, no reason exists to suspect that it dominates the low-level of live–dead discordance observed in these Arctic assemblages.

A larger concern, typically ignored in taphonomic analyses, is the effect of predation on benthic prey, which in DBO1 is both well-studied and intense. For example, the DBO1 region is home to large populations of benthivorous Pacific walrus (*Odobenus rosmarus divergens*), which excavate a track of pits while hunting for infaunal prey (Oliver *et al.* 1983; Born *et al.* 2003; Ray *et al.* 2006). These excavations vary in length but average 0.4 m wide and are up to 0.2 m deep. Walrus are thus a major agent of large-scale bioturbation in the region, disturbing 2–3% of Bering and Chukchi seabed in a five-month summer season, and their feeding traces have been suggested as contributing to the extremely high benthic productivity on the Pacific Arctic Shelf by releasing nutrients and creating habitat heterogeneity (Ray *et al.* 2006). When feeding, walruses jet water into the seabed to loosen it, but do not shift large volumes: when a prey item is found, the soft tissues are stripped from the shells, which are left behind in the seabed with re-settled sediment (Oliver *et al.* 1983; Ray *et al.* 2006). Both shell and sediment movement are thus very localized, and so postmortem transport between habitats should be negligible despite the large populations of walrus. Considering postmortem loss rates of shells, it is possible that walruses increase aragonitic shell loss through their irrigation of the surface mixed layer with well-oxygenated and cold, slightly undersaturated water,

aggravating the undersaturation of porewaters created by aerobic decomposition. However, this process would apply to the entire dead-shell assemblage and across the entire study area: bias would arise from interspecies differences in the inherent durability of shells, as already discussed (and rejected), not from direct walrus predation.

In contrast, the DBO1 region is also the seasonal feeding area of large populations of benthivorous spectacled eider (*Somatera fuscgeri*), and their net effects are harder to reject. While in the northern Bering Sea, these birds eat specific size classes of infaunal deposit-feeding bivalves, especially Nuculanidae (*Nuculana radiata*) along with smaller numbers of Nuculidae (*Ennucula tenuis*) and Tellinidae (*Macoma* spp.; Lovvorn *et al.* 2003). These birds preferentially ingest – and pulverize the shells of – individuals in the 18–24 mm size range, while some smaller individuals pass through the gut without damage (or death), and larger specimens are rejected. Fragmentary remains of predated bivalves are then deposited on ice flows directly above the feeding grounds (Petersen *et al.* 2000), with potential to settle back to the seabed, although probably not in a taxonomically identifiable condition. This intense, selective removal of living individuals from the community would also cause a comparable number of their shells to fail to enter the death assemblage; these target taxa (mostly Nuculanidae) should thus be under-represented in death assemblages. Instead, we found that the 2014 death assemblages were enriched rather than depleted in Nuculanidae relative to living assemblages throughout the 2000–14 time-series, and can affirm that large numbers of *Nuculana radiata* in the targeted 18–24 mm size class were sampled both alive and dead at all five SLIP sites during that period. The preferred prey was thus not removed entirely from benthic communities by predation nor erased from the death assemblage, and in fact the observed live–dead contrast (more abundant dead than alive) is opposite to that predicted from a predation bias against preservation. We thus reject H4 to explain observed live–dead discordance.

We note that an ecologically-driven change (H5) in taphonomic conditions could have occurred if, within the window of time-averaging, the intensity of eider predation changed. However, based on the populations that could be estimated on sea ice during the winter or at Alaskan nesting regions in spring, spectacled eiders are judged to be vulnerable but stable from 1995 to 2010 (Petersen *et al.* 1999; Petersen and Douglas 2004; Larned *et al.* 2012; Fischer *et al.* 2017), overlapping with our study interval. We thus suspect no taphonomic bias (H4), nor ecologically driven change in bias (H5), against the preservation of *Nuculana radiata* related to duck predation. The dominance of Nuculanidae in the death assemblages of all five SLIP sites is thus likely a faithful signal from its past abundance alive (see H5).

H5: live–dead differences arise from ecological change within the window of time-averaging

It could be argued that ecological change within the window of time-averaging (H5 in Table 4) is the most likely explanation for observed levels of live–dead discordance in sandy mud and mud seabeds of DBO1; simply given our ability to reject, or at least doubt the adequacy of, the alternative hypotheses H1–4. Fortunately, the exceptional availability of a 15-year time-series of living data (Figs 3 & 4) as well as data from earlier cruises (discussed below) means that we can test H5 explicitly. If H5 is true, then death assemblages should (a) exhibit the greatest discordance with the most recently-collected living assemblage, and either (b) agree most closely with the oldest-collected live data or (c) have a composition that is intermediate between the oldest and most recent sampling, consistent with time-averaging of shell input over an interval including a strong shift in the ecological baseline.

We found that the death assemblage is most discordant with the youngest-collected living assemblage in most comparisons (option a), in both the sandy mud and mud habitats and whether analyses were performed at the guild- or family-level. Discordance was greatest in sites from sandy mud seabeds (SLIP1–3, Figs 9a, 10 & 11), where the family-level composition of the bivalve living assemblages is known to have changed most strongly and most steadily (Fig. 3). In particular, the overabundance of Nuculanidae in the death assemblage (Fig. 11) is consistent with the documented decline in that family over the 15-year living time-series (Figs 3 & 5a). In contrast, mud stations (SLIP4–5) exhibit less strong live–dead discordance (Figs 8 & 9b), commensurate with the smaller changes in composition of the living assemblage within the 15-year time-series there (Figs 3 & 5b). Death assemblages have a composition that either most closely resembles the earliest sampling of the living assemblages (SLIP5) or is intermediate to early and later samples (option c above), depending on the test. However, Nuculanidae is again overabundant in the death assemblage, consistent with their documented trend in living assemblages.

Biomonitoring trends from 2000 to 2014 thus support the ecological change that would be inferred from the observed live–dead discordance, namely a strong decline in the obligate deposit-feeding Nuculanidae throughout DBO1. Biomonitoring time-series like those discussed here are relatively

rare in other areas of the Arctic, or the continental shelf at large. Therefore, if changes in seafloor community composition could be correctly inferred from a single sampling year of live and dead data then this method would prove a reliable means of gathering historical biological data on the recent past in the Arctic and other seabeds. When we evaluate a single year of live and dead data in DBO1 (2014 live and dead; and for a biomass-based comparison, see Meadows *et al.* 2019), we find that we would correctly infer that the decline in Nuculanidae had been accompanied by proportional increases in the smaller-bodied obligate deposit-feeding Nuculidae and in the mixed-feeding Tellinidae in the sandy mud habitat, as evident in the living time-series (Fig. 3). At the guild-level (Figs 3 & 8a), we would also correctly recognize a decline in the proportional importance of obligate deposit-feeders at the expense of mixed feeders in the sandy mud habitat. In the mud habitat, we would correctly infer that the proportional decline in Nuculanidae was countered by a strong proportional increase in Nuculidae and a relatively steady proportion of Tellinidae, consistent with the living time-series (Fig. 3), and would also correctly recognize the much smaller change in feeding guilds than in the muddy sand habitat (Fig. 8a). The test of H5 using the live time-series is thus, at a first order, strongly affirmative using both guild- and family-level proportional abundance data, and points to the broad value of live–dead comparison even using a single year of sampling.

Owing to time-averaging, death assemblages typically contain many specimens that pre-date the recent onset of benthic monitoring, and our preliminary age-dating of shells indicates that this is probably also true in the DBO1 region (see H3 above; shells up to a few centuries old). The high proportional abundance of Nuculanidae, which in death assemblages at all sites is higher than encountered in any single living assemblage between 2000 and 2014 (Fig. 3), may thus reflect a shell input from an earlier period of even higher dominance by that family. Indeed, compositional data from earlier surveys document a steady and significant decline in Nuculanidae as a proportion of total macrobenthic biomass from the mid-1980s to the 2000s, declining from *c.* 70% to <50% (Fig. 13; Grebmeier 2012). Comparing the part of this biomass-based trend (Fig. 13) that overlaps with the 15 years of numerical abundance data used here (Figs 3 & 5) shows that the decline in Nuculanidae is robust to units of measurement. The overabundance of Nuculanidae in death assemblages within DBO1 is thus a meaningful record of its formerly higher abundance in this region: the death assemblage detects a biological trend that started before the onset of biomonitoring.

It is also important to note what live–dead comparison cannot detect readily, namely the changes in *absolute* abundance that lie behind the changes in proportional abundance analysed here. For example, at the muddy sand sites (SLIP1–3), we would not appreciate that the proportional decline in Nuculanidae involved a strong, almost order-of-magnitude decline in its absolute abundance; that the proportional increase in Nuculidae reflected a genuine increase in its density (as opposed to steady populations in the face of declining Nuculanidae); nor that Yolidiidae experienced a recent pulse in density (Fig. 5a). Similarly, at the mud sites (Fig. 5b), we would not be able to detect that the density of both Nuculanidae and Nuculidae had been in decline at SLIP5 and had simply switched ranks during that decline, in contrast to their opposing trajectories at SLIP4 (where trends are more like those at the sandy mud sites). Because changes in the raw abundance of taxa can alter local rates of shell input to the seabed, we discuss their taphonomic implications below.

Facies-level differences influenced by rates of shell input

Palaeoecological interpretation tends to assume no change in rates of shell input over time, i.e. that each past cohort had an equal chance of representation in the ultimate, time-averaged assemblage, even though it is expected (and generally concluded) that taphonomic loss weakens the signal from the earlier phases, all else being equal (Tomašových *et al.* 2014, 2016). Where ecological conditions have changed during the window of shell accumulation, we also allow that those changes might have entailed a shift in total input – not just in the proportional representation of species – and/or a shift in

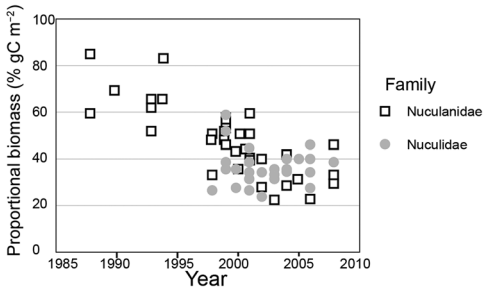

Fig. 13. Significant decline since the 1980s in Nuculanidae bivalves, a preferred prey item for spectacled eider, as a proportion of total macrobenthic biomass at SLIP1–5. Source: modified from Grebmeier (2012).

the inherent preservation potential of shell input (e.g. owing to a change in shell mineralogy or body size), and/or change in taphonomic conditions (e.g. predation intensity, water saturation state, as discussed under H4). Change in the net rate of shell input, or inherent durability of those shells – both are ecological changes (H5) – would lead to the under- or over-representation of some phases, affecting the rate at which the composition of the dead-shell assemblage adjusts toward that of the youngest living assemblages (i.e. affecting taphonomic inertia; Kidwell 2007, 2008). If shell input from the new community state is at a higher rate or more inherently durable, then that input can more quickly shift the death assemblage away from its long-term composition accrued from earlier community state(s), making it resemble the 'new' community more closely than otherwise expected.

In DBO1, such dynamics probably applied, although differently among sites owing to differences in total bivalve living density (dashed grey lines in Fig. 5). In both sandy mud and mud sites, the relatively thick-shelled Nuculanidae disproportionately dominates death assemblages (Fig. 3). Nuculanidae also dominated bivalve living communities throughout DBO1 during the 1980s based on earlier surveys but declined through the 1990s and the 2000–14 time-series used here (Figs 3 & 13; Grebmeier *et al.* 1989, 2018). The high abundance of Nuculanidae in death assemblages sampled in 2014 is thus a memory of the decline in this group. In the sandy mud habitat (SLIP1–3), the strength of this signal of decline – i.e. the magnitude of live–dead discordance – is relatively strong, perhaps because *total* bivalve abundance here either *changed very little or declined only slightly* between 2000 and 2014 (Fig. 8a). In contrast, living density *increased* strongly at SLIP4 in the mud habitat, perhaps explaining why that death assemblage resembles intermediate-age living assemblages more strongly than it does the oldest living assemblages, despite the ecological change coming largely from an absolute increase in thin-shelled Tellinidae. Finally, living bivalve density at SLIP5 *decreased* strongly and the death assemblage resembles most closely the oldest living assemblages, like death assemblages from the sandy mud habitat where total input also declined or was steady. At SLIP5, Tellinidae declined in absolute abundance despite rising in dominance, and thus their shells fail to register strongly, perhaps exaggerated by a lower preservation potential. Changes in rates of shell input, which are implicit from changes in bivalve living density, can thus explain second-order variation in live–dead discordance between the sandy mud sites and mud sites, with possible amplification by family-level differences in preservability related to shell thickness.

The effect of ecological changes in body size could also amplify – or suppress – live–dead discordance. We do not have body size data but can calculate the average mass of an individual using per-family data on biomass (gC m^{-2}) and numbers of individuals (annual data per station; Fig. 14). We find that Nuculanidae were, on average across all years 2000–14, larger bodied in the sandy mud habitat (0.023–0.026 gC/individual at SLIP1–3) than in the mud habitat (0.0047–0.0055 gC/individual, SLIP4–5; two-sample unpaired *t*-test on Nuculanidae estimated individual size per station per year yielded p-value <0.0001). The net effect of this habitat-level difference would be to diminish live–dead discordance in the mud habitat, assuming that the input of smaller-bodied Nuculanidae shells would cause them to become less well represented in the mud death assemblage than the comparatively larger-bodied shells input to the sandy mud death assemblage. Temporally, Nuculanidae declined in body size in 2012–14 at SLIP1 (not shown in Fig. 14), but otherwise varied little: if smaller specimens have lower preservation potential, then the net effect of this diminution in size would be to suppress the live–dead contrast at SLIP1. The sandy mud habitat does indeed exhibit a stronger live–dead contrast, as predicted by both of these patterns in body size, although we believe that the observed discordance arises primarily from the declining proportional abundance of living Nuculanidae (see H5 above) and the absolute decline in the population size (i.e. shell input in terms of numbers of individuals, this section of discussion). Body sizes of the other key families do not differ notably at a habitat scale, nor over time (Fig. 14). Nuculidae is small (0.006 gC/individual) at two muddy sand sites but its size at the third sandy mud site resembles that at the two mud sites (0.014 gC/individual at SLIP1 v. 0.010 and 0.018). Average Tellinidae body size shows little variation among sites (0.013–0.016 gC/individual) except for relatively small individuals at SLIP1 (0.007 gC/individual).

Overall, differences in the composition of living and death assemblages are thus easy to relate to known differences in recent biological history (H5) of these two habitats, but the discordance is amplified somewhat by changes in shell input (numbers of individuals) that are part of the ecological change (thus also H5). Death assemblages at sandy mud sites indeed bear a strong, preferential signal from the earliest-documented living assemblage (2000–04; Nuculanidae dominance, which was even higher in the 1980s, Fig. 13), strengthened by a decrease in total bivalve input over the 2000–14 time-series, whereas death assemblages from the mud stations tend to have compositions intermediate to the earliest and most-recent samplings of living assemblages,

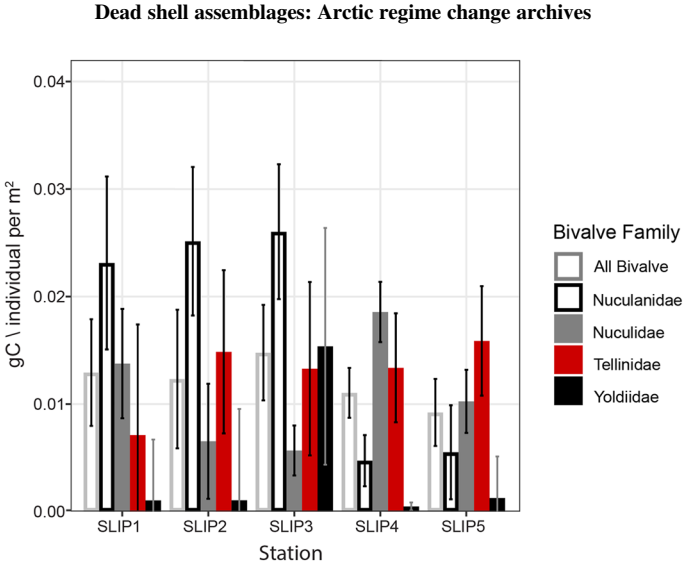

Fig. 14. Average biomass (gC) per individual for the major families, by station after summing individuals and biomass across all years. The average biomass of a bivalve individual across all families (grey outlined columns) is slightly higher in the sandy mud habitat (SLIP1–3) than in the mud habitat (SLIP4–5). Nuculanidae (black outlined columns) are consistently larger bodied in sandy muds than in muds, but the other key families do not differ strongly in body size at the habitat level, only site to site.

especially at SLIP4 (Fig. 8b) where total shell input increased over time.

Broader implications: detecting climate-related regime change in Arctic seabeds

Differences between sandy mud and mud middle-shelf death assemblages within DBO1 reflect the particular and disparate ecological changes that have occurred in these two habitats during a 'regime change' associated with deterioration of the Arctic cold-water front (Grebmeier *et al.* 2006, 2018; Fig. 1), rather than reflecting facies-level taphonomic differences (H5 rather than H4 in Table 4). The contrasts that exist in live–dead discordance between sandy mud and mud habitats in DBO1 should thus not be construed as general to these facies or elsewhere within the Arctic. However, our analysis does indicate the high degree to which time-averaged death assemblages can reflect past ecological input at a station scale in contrast to the many findings of fidelity at the coarser facies- and gradient-scales, especially in subtidal settings (e.g. reviewed by Kidwell and Tomašových 2013; LeClaire *et al.* 2022). This fidelity to local history is notwithstanding the rigors of postmortem preservation presented by cold, highly productive marine waters, which are here superimposed on the intense bioturbation and relatively slow net sedimentation typical of normoxic continental shelves.

Our analysis also shows that this spatial and compositional fidelity is robust to strong temporal changes in total bivalve abundance, including between-site differences within habitats, that would have altered rates of shell input (Fig. 5). More generally, the net rate of shell input might be affected by change(s) in the absolute abundance of shell-producing taxa (as definite here), the inherent durability of the new dominants (possible here, but with less-durable new dominants), and/or new taphonomic conditions (e.g. an increase in predation, bioturbation, or sedimentation that accompanies, or drives, community change). For example, the original global meta-analysis of live–dead datasets behind this approach recognized live–dead discordance associated with anthropogenic eutrophication, including that high discordance was almost certainly amplified by the rise to dominance of mostly thin-shelled organic-loving taxa over earlier community states characterized by diverse but mostly thicker-shelled oligotrophic bivalves (Kidwell 2007). The opposite situation is easily imagined, with shell production (or shell preservation) being higher for the new community state for some reason, diluting the signal from the earliest cohorts in the death assemblage more quickly than had net shell input rates remained constant. Such a dynamic likely figures in the muted live–dead contrast at SLIP4, where bivalve biomass and bivalve numerical abundance (Fig. 4b) are known to have increased over time, suppressing live–dead discordance using the more

recently sampled living assemblages. This contrasts with the dynamic at sandy mud sites SLIP1–3 and mud site SLIP5, where bivalve biomass declined in density in favour of polychaetes (Grebmeier *et al.* 2006) and numerical abundance either did not trend or declined, thus amplifying live–dead discordance in the same comparisons. Additional studies in regions with well-documented ecological histories, especially with data on biomass and the entire macrobenthic fauna such as available here, will help build a fully general model for the ecological interpretation of live–dead discordance, inclusive of non-constant rates of shell input.

We were surprised by the relatively poor performance of cross-plots of taxon presence–absence (Jaccard–Chao index) and rank-abundance (Spearman ρ) metrics in the DBO1 region, given strong temporal changes in the dominance of families (e.g. Fig. 3). Contrary to expectation, most live–dead comparisons fell into the upper-right quadrant of the cross-plot, indeed the extreme upper part of that quadrant with exceptional taxonomic similarity (Fig. 9). Meta-analytically, this is the quadrant where datasets from pristine, unmodified study systems typically fall when using habitat-level live–dead data, that is, where live and dead data from multiple sites have first been pooled at a facies scale (original method of Kidwell 2007, 2013); live–dead divergence of this scale can usually be explained by time-averaging alone. We used site-level data in DBO1, which makes the strong levels of Jaccard–Chao live–dead agreement at DBO1 sites even more remarkable. Researchers using site-level data commonly find a wide range of values down to low taxonomic similarity and, occasionally, negative rank-order correlations, with discordance attributable to a wide range of stressors (Yanes 2012; Chiba and Sato 2013; Michelson and Park 2013; Korpanty and Kelley 2014; Albano *et al.* 2016; Gilad *et al.* 2018).

Instead, throughout DBO1, live–dead discordance was most readily detected using measures that rely upon differences in proportional abundance of taxa, namely Pearson correlations (Fig. 8) and NMDS (Figs 10–12), implying that the response of the *bivalve* community to climate-related environmental changes, although significant, is not as acute as that of molluscs to other (spatially or temporally more acute) stressors elsewhere. The need for proportional abundance data to detect community change here might also arise at least in part from the relatively low richness of the bivalve fauna, which reduces the number of pairwise comparisons in a Spearman rank-order test and thus reduces the magnitude of rank change that is possible. Our use of families rather than species would have aggravated this effect. In response to stress, taxa (here families) shifted slightly in rank between living and dead but did not switch from being top-ranked to being low mid-ranked, rare, or absent the way taxa can within more taxon-rich samples. Many other assemblage-level analyses have also relied upon proportional abundance data to test for ecological stability, using live–dead cross-plots and multivariate displays (e.g. death assemblages falling entirely within the cloud of living assemblages, Martinelli *et al.* 2016) and change in response to eutrophication (Leshno *et al.* 2015), invasives (e.g. unusual trait-based analysis of Steger *et al.* 2022), climate change (e.g. biomass-based changes; Meadows *et al.* 2019), and multiple human stressors (Albano and Sabelli 2011; Haselmair *et al.* 2021).

We emphasize that the ecosystem-wide regime change recognized in DBO1 (Grebmeier *et al.* 2006) is expressed by many variables, including a shift from bivalve to polychaetae dominance in the macrobenthos that could not be detected via live–dead analysis of shelled fauna alone. Bivalve taxa themselves tended to shift between adjacent ranks rather than more strongly, with few live-only or dead-only taxa other than among the rarest groups. Strong interannual variability in those living assemblages (Fig. 4), another signifier of regime change, moreover produced a death assemblage with fairly equitable abundances among these switching dominants. The only other molluscan live–dead analyses focused on biotic response to climate change that we are aware of (other than Meadows *et al.* 2019) is that of Powell *et al.* (2017), who used disparities in the bathymetric distribution of living and dead individuals of two commercial bivalves, rather than a community-level analysis as here.

Additional tests of the power of live–dead analysis to detect biotic response to climate change are thus much needed, especially in polar settings where warming is amplified. It is important to realize that the immediate driver of biotic response in a subtidal setting, such as in DBO1, might be a change in mean temperature but is as likely to be a change in minimum temperature or temperature variability, upwelled nutrients, grain size related to current strength, oxygen, and/or planktic-benthic flux. Responses can thus be contrary to those predicted by mean temperature alone and, of course, can involve parts of the community lacking shelled hardparts and thus fall outside the domain of live–dead analysis.

Conclusions

These results are very encouraging regarding Arctic dead-shell assemblages as reliable archives of community composition and community change over the recent past. Notwithstanding the especially rigorous postmortem conditions expected in such cold

seabeds, death assemblage samples provided by van Veen grabs in DBO1 were fully adequate in size (Hypothesis 1) and their compositions have not been overtly biased by taphonomic processes (H3), nor do we have reason to suspect direct human modification of death assemblages (H2). Instead, DBO1 death assemblages detect the changes in community composition (H5) at both the guild and family-level that are known from biomonitoring, including site-level differences within the most organic-rich mud facies of the DBO1 hotspot (SLIP4 v. SLIP5). This resolution benefits from a likely very short window of time-averaging throughout this region (<200 years, H4), based on our preliminary shell age-dating work. The biological and physical rigors of the post-mortem environment have in fact likely shortened the memory of the death assemblage, allowing for easier detection of change occurring within recent decades.

The scatter of values of live–dead agreement produced by site-level data here and elsewhere can, of course, be attributable to random, single-sample variability in the living assemblage (i.e. noise), which is why habitat-level datasets that pool multiple spatial samples are most conservative in tests for live–dead discordance (Kidwell 2007; Michelson *et al.* 2018). However, we suspect that such site-level variation in live–dead discordance – whether evident in a coarse JC–ρ cross-plot or using NMDS or some other method exploiting proportional abundance data – is commonly an expression of the genuinely spatially pixelated dynamic by which a biota changes from one community state to another as opposed to spatially monotonic and gradual change across a habitat or landscape. That said, this study finds that community-level biotic response to ecosystem regime change driven by anthropogenic climate change – the confident stressor in DBO1 – is largely too subtle to detect with the coarse tools of taxon presence–absence and rank-abundance (JC–ρ) that are so effective in live–dead analysis where the spatial or temporal stress gradient is steeper. This result contrasts with the successful detection of bathymetric and other spatial shifts in *single* taxa using presence–absence data (e.g. Miller *et al.* 2013; Powell *et al.* 2017).

Climate-associated community-wide changes might in general require live–dead comparison focused on proportional numerical abundance, as here, and, to better coordinate with ecosystem scientists, measures of biomass (as explored in Meadows *et al.* 2019). Given that marine regime change is suspected to now be underway throughout the Arctic, these positive results from the Alaskan Arctic should motivate additional tests in high latitude seabeds, where molluscan dead-shell assemblages might become a valuable new means for detecting transitioning regions. Indeed, live–dead analysis could be used at the initiation of a monitoring effort to identify where the benthos is already in transition.

Acknowledgments We thank Eric Powell and an anonymous reviewer for their helpful comments; the crew and scientists onboard the CGC *Sir Wilfrid Laurier* 2014 cruise for their work over the summer of 2014; Linton Beaven, Stephanie Soques and Christina Goethel for work in the benthic sorting lab at the Chesapeake Biological Laboratory (CBL), along with data formatting and collaborative conversations with Alynne Bayard and Lee Cooper respectively, also at CBL; and students Kenzo Esquivel, Eva Haraldsdottir, and Lilja Carden for lab assistance at the University of Chicago. We also appreciate the collaboration of Adam Tomašových (Slovak Academy of Sciences) and Darrell Kaufman (University of Arizona) on related work mentioned here, and illuminating conversations with Max Hoberg (University of Alaska, Fairbanks), Monika Kędra (Institute of Oceanology PAN Powstańców Warszawy, Poland), and David Jablonski (University of Chicago).

Competing interests The authors declare that they have no known competing financial interests or personal relationships that could have appeared to influence the work reported in this paper.

Author contributions **CAM**: conceptualization (equal), data curation (equal), formal analysis (lead), funding acquisition (supporting), investigation (lead), methodology (equal), project administration (equal), resources (equal), validation (lead), visualization (lead), writing – original draft (equal), writing – review & editing (lead); **JMG**: data curation (equal), formal analysis (supporting), funding acquisition (equal), methodology (equal), resources (equal), writing – review & editing (equal); **SMK**: conceptualization (equal), formal analysis (supporting), funding acquisition (equal), investigation (supporting), methodology (equal), project administration (equal), resources (equal), validation (supporting), visualization (supporting), writing – original draft (equal), writing – review & editing (equal).

Funding The study was supported by grants from the Paleontological Society and Geological Society of America (to CAM), US National Science Foundation Arctic Observing Network grant ARC-1204082 and 1917469 (to JMG and LWC), and the American Chemical Society Petroleum Research Fund ACS PRF# 58795-ND8 (to SMK), whose donors are gratefully acknowledged

Data availability The full biological and environmental datasets used here are not yet publicly available because they are not yet fully integrated into the NSF Arctic Data Center. The bivalve dead datasets used here are available from the corresponding author. All other datasets are cited and available in the NSF Arctic Data Center.

References

Albano, P.G. and Sabelli, B. 2011. Comparison between death and living molluscs assemblages in a Mediterranean infralittoral off-shore reef. *Palaeogeography, Palaeoclimatology, Palaeoecology*, **310**, 206–215, https://doi.org/10.1016/j.palaeo.2011.07.012

Albano, P.G., Filippova, N., Steger, J., Kaufman, D.S., Tomašových, A., Stachowitsch, M. and Zuschin, M. 2016. Oil platforms in the Persian (Arabian) Gulf: living and death assemblages reveal no effects. *Continental Shelf Research*, **121**, 21–34, https://doi.org/10.1016/j.csr.2015.12.007

Albano, P.G., Gallmetzer, I., Haselmair, A., Tomašových, A., Stachowitsch, M. and Zuschin, M. 2018. Historical ecology of a biological invasion: the interplay of eutrophication and pollution determines time lags in establishment and detection. *Biological Invasions*, **20**, 1417–1430, https://doi.org/10.1007/s10530-017-1634-7

Aller, R.C. 1982. The Effects of Macrobenthos on Chemical Properties of Marine Sediment and Overlying Water. *Topics in Geobiology*, 53–102, https://doi.org/10.1007/978-1-4757-1317-6_2

Arkle, K.M. and Miller, A.I. 2018. Evidence for stratigraphy in molluscan death assemblages preserved in seagrass beds: St. Croix, U.S. Virgin Islands. *Paleobiology*, **44**, 155–170, https://doi.org/10.1017/pab.2017.26

Becker, S. 2015. *Recommended Protocols for Sampling and Analyzing Subtidal Benthic Macroinvertebrate Assemblages in Puget Sound*. Report No. 15-09-046, Puget Sound Esuary Protocols, 980. Department of Ecology, EPA, and Puget Sound Water Quality Authority, Olympia, Washington, USA, https://apps.ecology.wa.gov/publications/SummaryPages/1509046.html

Blanchard, A.L. 2014. Variability of macrobenthic diversity and distributions in Alaskan sub-Arctic and Arctic marine systems with application to worldwide Arctic Systems. *Marine Biodiversity*, **45**, 781–795, https://doi.org/10.1007/s12526-014-0292-6

Blanchard, A.L. and Feder, H.M. 2014. Interactions of habitat complexity and environmental characteristics with macrobenthic community structure at multiple spatial scales in the northeastern Chukchi Sea. *Deep Sea Research Part II: Topical Studies in Oceanography*, **102**, 132–143, https://doi.org/10.1016/j.dsr2.2013.09.022

Borcard, D., Gillet, F. and Legendre, P. 2011. *Numerical Ecology with R*. Springer Science and Business, New York, https://doi.org/10.1007/978-1-4419-7976-6

Born, E.W., Rysgaard, S., Ehlmé, G., Sejr, M., Acquarone, M. and Levermann, N. 2003. Underwater observations of foraging free-living Atlantic walruses (*Odobenus rosmarus rosmarus*) and estimates of their food consumption. *Polar Biology*, **26**, 348–357, https://doi.org/10.1007/s00300-003-0486-z

Brown, G.M. and Larina, E. 2019. Environmental controls on shallow subtidal molluscan death assemblages on San Salvador Island, The Bahamas. *Palaeogeography, Palaeoclimatology, Palaeoecology*, **527**, 14–24, https://doi.org/10.1016/j.palaeo.2019.04.019

Casebolt, S. and Kowalewski, M. 2018. Mollusk shell assemblages as archives of spatial structuring of benthic communities around subtropical islands. *Estuarine, Coastal and Shelf Science*, **215**, 132–143, https://doi.org/10.1016/j.ecss.2018.09.023

Chao, A., Chazdon, R.L., Colwell, R.K. and Shen, T. 2005. A new statistical approach for assessing similarity of species composition with incidence and abundance data. *Ecology Letters*, **8**, 148–159, https://doi.org/10.1111/j.1461-0248.2004.00707.x

Chiba, T. and Sato, S. 2013. Invasion of *Laguncula pulchella* (Gastropoda: Naticidae) and predator–prey interactions with bivalves on the Tona coast, Miyagi prefecture, northern Japan. *Biological Invasions*, **15**, 587–598, https://doi.org/10.1007/s10530-012-0310-1

Coan, E.V., Scott, P.V. and Bernard, F.R. 2000. *Bivalve Seashells of Western North America*. 1st edn. Santa Barbara Museum of Natural History Monographs; Studies in Biodiversity, Santa Barbara, California.

Cooper, L.W. and Grebmeier, J.M. 2018. Deposition patterns on the Chukchi shelf using radionuclide inventories in relation to surface sediment characteristics. *Deep Sea Research Part II: Topical Studies in Oceanography*, **152**, 48–66, https://doi.org/10.1016/j.dsr2.2018.01.009

Cooper, L.W., Sexson, M.G., Grebmeier, J.M., Gradinger, R., Mordy, C.W. and Lovvorn, J.R. 2013. Linkages between sea-ice coverage, pelagic–benthic coupling, and the distribution of spectacled eiders: observations in March 2008, 2009 and 2010, northern Bering Sea. *Deep Sea Research Part II: Topical Studies in Oceanography*, **94**, 31–43, https://doi.org/10.1016/j.dsr2.2013.03.009

Creamean, J.M., Cross, J.N. *et al*. 2019. Ice nucleating particles carried from below a phytoplankton bloom to the Arctic atmosphere. *Geophysical Research Letters*, **46**, 8572–8581, https://doi.org/10.1029/2019GL083039

Cross, J.N., Mathis, J.T., Pickart, R.S. and Bates, N.R. 2018. Formation and transport of corrosive water in the Pacific Arctic region. *Deep Sea Research Part II: Topical Studies in Oceanography*, **152**, 67–81, https://doi.org/10.1016/j.dsr2.2018.05.020

Dufour, S.C. 2005. Gill anatomy and the evolution of symbiosis in the bivalve Family Thyasiridae. *The Biological Bulletin*, **208**, 200–212, https://doi.org/10.2307/3593152

Emerson, S.R., Archer, D., Charnock, H., Edmond, J.M., McCave, I.N., Rice, A.L. and Wilson, T.R.S. 1990. Calcium carbonate preservation in the ocean. *Philosophical Transactions of the Royal Society of London, Series A, Mathematical and Physical Sciences*, **331**, 29–40, https://doi.org/10.1098/rsta.1990.0054

Ferguson, C.A. 2008. Nutrient pollution and the molluscan death record: use of mollusc shells to diagnose environmental change. *Journal of Coastal Research*, **24**, 250–259, https://doi.org/10.2112/06-0650.1

Fischer, J.B., Williams, A.R. and Stehn, R.A. 2017. *Nest Population Size and Potential Production of Geese and Spectacled Eiders on the Yukon-Kuskokwim Delta, Alaska, 1985-2016*. Technical Report, US Fish and Wildlife Service, Migratory Bird Management, Anchorage, Alaska, USA, https://www.fws.gov/r7/mbsp/mbm/waterfowl/surveys/pdf/2016_YKD_Nest_Plot_Survey.pdf

Flessa, K.W. 1998. Well-traveled cockles: shell transport during the Holocene transgression of the southern

North Sea. *Geology*, **26**, 187–190, https://doi.org/10.1130/0091-7613(1998)026<0187:WTCSTD>2.3.CO;2

Foster, N.R. 1991. *Intertidal Bivalves: a Guide to the Common Marine Bivalves of Alaska*. University of Alaska Press, Fairbanks, Alaska, USA.

Gallmetzer, I., Haselmair, A., Tomašových, A., Stachowitsch, M. and Zuschin, M. 2017. Responses of molluscan communities to centuries of human impact in the northern Adriatic Sea. *PLOS ONE*, **12**, e0180820, https://doi.org/10.1371/journal.pone.0180820

Gee, G.W. and Bauder, J.W. 1986. Particle-size analysis. *In*: Klute, A. (ed.) *Methods of Soil Analysis*. Soil Science Society of America, 383–411, https://doi.org/10.2136/sssabookser5.1.2ed.c15

Gilad, E., Kidwell, S.M., Benayahu, Y. and Edelman-Furstenberg, Y. 2018. Unrecognized loss of seagrass communities based on molluscan death assemblages: historic baseline shift in tropical Gulf of Aqaba, Red Sea. *Marine Ecology Progress Series*, **589**, 73–83, https://doi.org/10.3354/meps12492

Gill, M.J., Crane, K. *et al*. 2011. Arctic Marine Biodiversity Monitoring Plan (CBMP-MARINE PLAN). CAFF Monitoring Series Report No. 3, April 2011, CAFF International Secretariat, Akureyri, Iceland.

Glover, C.P. and Kidwell, S.M. 1993. Influence of organic matrix on the post-mortem destruction of molluscan shells. *The Journal of Geology*, **101**, 729–747, https://doi.org/10.1086/648271

Grebmeier, J.M. 2012. Shifting patterns of life in the Pacific Arctic and sub-Arctic seas. *Annual Reviews in Marine Science*, **4**, 63–78, https://doi.org/10.1146/annurev-marine-120710-100926

Grebmeier, J.M. and Cooper, L.W. 1995. Influence of the St. Lawrence Island polynya upon the Bering Sea benthos. *Journal of Geophysical Research: Oceans*, **100**, 4439–4460, https://doi.org/10.1029/94JC02198

Grebmeier, J.M. and Cooper, L. 2016*a*. *PacMARS Surface Sediment Parameters (1970–2012)*. NSF Arctic Data Center, https://doi.org/10.5065/D6416V3G

Grebmeier, J.M. and Cooper, L.W. 2016*b*. The Saint Lawrence Island Polynya: a 25-year evaluation of an analogue for climate change in Polar Regions. *In*: Gilbert, P. and Kana, T. (eds) *Aquatic Microbial Ecology and Biogeochemistry: A Dual Perspective*. Springer, Cham, 171–183, https://doi.org/10.1007/978-3-319-30259-1_14

Grebmeier, J.M. and Cooper, L.W. 2018. *SWL13 Sediment Parameters*. NSF Arctic Data Center, https://doi.org/10.5065/D63X84PT

Grebmeier, J.M. and Cooper, L.W. 2019*a*. Benthic macroinfaunal samples collected from the Canadian Coast Guard Ship (CCGS) Sir Wilfrid Laurier, Northern Bering Sea to Chukchi Sea, 2013, NSF Arctic Data Center, https://doi.org/10.18739/A2N29P67H

Grebmeier, J.M. and Cooper, L.W. 2019*b*. Surface sediment samples collected from the Canadian Coast Guard Ship (CCGS) Sir Wilfrid Laurier, Northern Bering Sea to Chukchi Sea, 2014, NSF Arctic Data Center, https://doi.org/10.18739/A2WH2DF2X

Grebmeier, J.M. and Cooper, L.W. 2020. *PacMARS Sediment Community Oxygen Uptake (1984-2012)*. NSF Arctic Data Center, https://doi.org/10.5065/D600004Q

Grebmeier, J.M., Feder, H.M. and McRoy, C.P. 1989. Pelagic–benthic coupling on the shelf of the northern Bering and Chukchi Seas. II. Benthic community structure. *Marine Ecology Progress Series*, **51**, 253–268, https://doi.org/10.3354/meps051253

Grebmeier, J.M., Overland, J.E. *et al*. 2006. A major ecosystem shift in the northern Bering Sea. *Science (New York, NY)*, **311**, 1461–1464, https://doi.org/10.1126/science.1121365

Grebmeier, J.M., Bluhm, B.A. *et al*. 2015*a*. Ecosystem characteristics and processes facilitating persistent macrobenthic biomass hotspots and associated benthivory in the Pacific Arctic. *Progress in Oceanography*, **136**, 92–114, https://doi.org/10.1016/j.pocean.2015.05.006

Grebmeier, J.M., Cooper, L.W. *et al*. 2015*b*. *Pacific Marine Arctic Regional Synthesis (PacMARS) Final Report*. Final Report, North Pacific Research Board, Washington, DC, USA, https://pacmars.cbl.umces.edu/Documents/PacMARS%20Final%20Report_2015.pdf

Grebmeier, J.M., Bluhm, B.A. *et al*. 2015*c*. Time-Series benthic community composition and biomass and associated environmental characteristics in the Chukchi Sea during the RUSALCA 2004–2012 Program. *Oceanography*, **28**, 116–133, https://doi.org/10.5670/oceanog.2015.61

Grebmeier, J.M., Frey, K.E., Cooper, L.W. and Kędra, M. 2018. Trends in benthic macrofaunal populations, seasonal sea ice persistence, and bottom water temperatures in the Bering Strait region. *Oceanography*, **31**, 136–151, https://doi.org/10.5670/oceanog.2018.224

Harper, E.M. 2000. Are calcitic layers an effective adaptation against shell dissolution in the Bivalvia? *Journal of Zoology*, **251**, 179–186, https://doi.org/10.1111/j.1469-7998.2000.tb00602.x

Haselmair, A., Gallmetzer, I., Tomašovỳch, A., Wieser, A.M., Übelhör, A. and Zuschin, M. 2021. Basin-wide infaunalisation of benthic soft-bottom communities driven by anthropogenic habitat degradation in the northern Adriatic Sea. *Marine Ecology Progress Series*, **671**, 45–65, https://doi.org/10.3354/meps13759

Hassan, G.S. 2015. On the benefits of being redundant: low compositional fidelity of diatom death assemblages does not hamper the preservation of environmental gradients in shallow lakes. *Paleobiology*, **41**, 154–173, https://doi.org/10.1017/pab.2014.10

Jiang, L., Feely, R.A., Carter, B.R., Greeley, D.J., Gledhill, D.K. and Arzayus, K.M. 2015. Climatological distribution of aragonite saturation state in the global oceans. *Global Biogeochemical Cycles*, **29**, 1656–1673, https://doi.org/10.1002/2015GB005198

Johannessen, O.M., Bengtsson, L. *et al*. 2004. Arctic climate change: observed and modelled temperature and sea-ice variability. *Tellus A*, **56**, 328–341, https://doi.org/10.1111/j.1600-0870.2004.00060.x

Kędra, M. and Oleszczuki, B. 2017. Pacific Arctic Benthic Species. http://www.iopan.gda.pl/projects/DBO/

Keil, R. 2017. Anthropogenic forcing of carbonate and organic carbon preservation in marine sediments. *Annual Review of Marine Science*, **9**, 151–172, https://doi.org/10.1146/annurev-marine-010816-060724

Kidwell, S.M. 2007. Discordance between living and death assemblages as evidence for anthropogenic ecological

change. *Proceedings of the National Academy of Sciences*, **104**, 17701–17706, https://doi.org/10.1073pnas.0707194104

Kidwell, S.M. 2008. Ecological fidelity of open marine molluscan death assemblages: effects of post-mortem transportation, shelf health, and taphonomic inertia. *Lethaia*, **41**, 199–217, https://doi.org/10.1111/j.1502-3931.2007.00050.x

Kidwell, S.M. 2013. Time-averaging and fidelity of modern death assemblages: building a taphonomic foundation for conservation palaeobiology. *Palaeontology*, **56**, 487–522, https://doi.org/10.1111/pala.12042

Kidwell, S.M. and Tomašových, A. 2013. Implications of time-averaged death assemblages for ecology and conservation biology. *Annual Review of Ecology, Evolution, and Systematics*, **44**, 539–563, https://doi.org/10.1146/annurev-ecolsys-110512-135838

Korpanty, C.A. and Kelley, P.H. 2014. Molluscan live–dead agreement in anthropogenically stressed seagrass habitats: siliciclastic v. carbonate environments. *Palaeogeography, Palaeoclimatology, Palaeoecology*, **410**, 113–125, https://doi.org/10.1016/j.palaeo.2014.05.014

Kowalewski, M., Casebolt, S., Hua, Q., Whitacre, K.E., Kaufman, D.S. and Kosnik, M.A. 2018. One fossil record, multiple time resolutions: disparate time-averaging of echinoids and mollusks on a Holocene carbonate platform. *Geology*, **46**, 51–54, https://doi.org/10.1130/g39789.1

Krause, R., Barbour, S., Kowalewski, M., Kaufman, D., Romanek, C., Simões, M. and Wehmiller, J. 2010. Quantitative comparisons and models of time-averaging in bivalve and brachiopod shell accumulations. *Paleobiology*, **36**, 428–452, https://doi.org/10.1666/08072.1

Larned, W., Bollinger, K. and Stehn, R. 2012. *Late Winter Population and Distribution of Spectacled Eiders (Somateria Fischeri) in the Bering Sea 2009 & 2010*. Project Report 820, US Department of Commerce, National Oceanic and Atmospheric Administration, as recommended by The North Pacific Research Board, Washington, DC, USA, https://www.fws.gov/r7/mbsp/mbm/waterfowl/surveys/pdf/spei_surveys_2009-10_report.pdf

LeClaire, A.M., Powell, E.N., Mann, R., Hemeon, K.M., Pace, S.M., Sower, J.R. and Redmond, T.E. 2022. Historical biogeographic range shifts and the influence of climate change on ocean quahogs (*Arctica islandica*) on the Mid-Atlantic Bight. *The Holocene*, **32**, 964–976, https://doi.org/10.1177/09596836221101275

Leonard-Pingel, J., Kidwell, S., Tomašových, A., Alexander, C. and Cadien, D. 2019. Gauging benthic recovery from twentieth century pollution on the southern California continental shelf using bivalves from sediment cores. *Marine Ecology Progress Series*, **615**, 101–119, https://doi.org/10.3354/meps12918

Leshno, Y., Edelman-Furstenberg, Y., Mienis, H. and Benjamini, C. 2015. Molluscan live and dead assemblages in an anthropogenically stressed shallow-shelf: Levantine Margin of Israel. *Palaeogeography, Palaeoclimatology, Palaeoecology*, **433**, 49–59, https://doi.org/10.1016/j.palaeo.2015.05.008

Lovvorn, J.R., Richman, S.E., Grebmeier, J.M. and Cooper, L.W. 2003. Diet and body condition of spectacled eiders wintering in pack ice of the Bering Sea. *Polar Biology*, **26**, 259–267, https://doi.org/10.1007/s00300-003-0477-0

Lovvorn, J.R., North, C.A., Grebmeier, J.M., Cooper, L.W. and Kolts, J.M. 2018. Sediment organic carbon integrates changing environmental conditions to predict benthic assemblages in shallow Arctic seas. *Aquatic Conservation: Marine and Freshwater Ecosystems*, **28**, 861–871, https://doi.org/10.1002/aqc.2906

Mann, R., Powell, E.N. and Munroe, D.M. 2020. The case of the 'missing' Arctic bivalves and the walrus: the biggest [overlooked] clam fishery on the planet. *Journal of Shellfish Research*, **39**, 501–509, https://doi.org/10.2983/035.039.0301

Martinelli, J.C., Madin, J.S. and Kosnik, M.A. 2016. Dead shell assemblages faithfully record living molluscan assemblages at One Tree Reef. *Palaeogeography, Palaeoclimatology, Palaeoecology*, **457**, 158–169, https://doi.org/10.1016/j.palaeo.2016.06.002

Mathis, J.T., Cross, J.N. and Bates, N.R. 2011. The role of ocean acidification in systemic carbonate mineral suppression in the Bering Sea. *Geophysical Research Letters*, **38**, L19602, https://doi.org/10.1029/2011GL048884

Mathis, J.T., Grebmeier, J.M. *et al*. 2014. Carbon biogeochemistry of the western Arctic: primary production, carbon export and the controls on ocean acidification. *In*: Grebmeier, J.M. and Maslowski, W. (eds) *The Pacific Arctic Region: Ecosystem Status and Trends in a Rapidly Changing Environment*. Springer, 223–268, https://doi.org/10.1007/978-94-017-8863-2_9

Meadows, C.A. 2020. *Community-Level Biotic Response to Increasing Climate Variability during the Last 150 Years: Steady and Warming Conditions on the Continental Shelf of the Pacific Arctic*. The University of Chicago, https://doi.org/10.6082/uchicago.2760

Meadows, C.A., Grebmeier, J.M. and Kidwell, S.M. 2019. High-latitude benthic bivalve biomass and recent climate change: testing the power of live–dead discordance in the Pacific Arctic. *Deep Sea Research Part II: Topical Studies in Oceanography*, **162**, 152–163, https://doi.org/10.1016/j.dsr2.2019.04.005

Meadows, C.A., Kidwell, S.M., Kaufman, D. and Tomašových, A. 2020. Calibration of aragonite shell loss rates and time-averaging in Arctic seabeds: benthic activity makes a tough situation tougher. *Geological Society of America Abstracts with Programs*. – GSA – GSA 2020 Connects Online, 6, https://doi.org/10.1130/abs/2020AM-355163

Michelson, A.V. and Park, L.E. 2013. Taphonomic dynamics of lacustrine ostracodes on San Salvador Island, Bahamas: high fidelity and evidence of anthropogenic modification. *PALAIOS*, **28**, 129–135, https://doi.org/10.2110/palo.2012.p12-031r

Michelson, A.V., Kidwell, S.M., Boush, L.E.P. and Ash, J.L. 2018. Testing for human impacts in the mismatch of living and dead ostracode assemblages at nested spatial scales in subtropical lakes from the Bahamian archipelago. *Paleobiology*, **44**, 758–782, https://doi.org/10.1017/pab.2018.20

Miller, J.H., Druckenmiller, P. and Bahn, V. 2013. Antlers on the Arctic Refuge: capturing multi-generational patterns of calving ground use from bones on the

landscape. *Proceedings of the Royal Society B: Biological Sciences*, **280**, 20130275, https://doi.org/10.1098/rspb.2013.0275

Moore, S.E. and Grebmeier, J.M. 2018. The Distributed Biological Observatory: linking physics to biology in the Pacific Arctic Region + Supplementary File (See Article Tools). *Arctic*, **71**, 1–7, https://doi.org/10.14430/arctic4606

Mueter, F.J. and Litzow, M.A. 2008. Sea ice retreat alters the biogeography of the Bering Sea continental shelf. *Ecological Applications*, **18**, 309–320, https://doi.org/10.1890/07-0564.1

Munroe, D.M., Powell, E.N., Mann, R., Klinck, J.M. and Hofmann, E.E. 2013. Underestimation of primary productivity on continental shelves: evidence from maximum size of extant surfclam (*Spisula solidissima*) populations. *Fisheries Oceanography*, **22**, 220–233, https://doi.org/10.1111/fog.12016

NOAA 2008. *Fisheries of the Exclusive Economic Zone Off Alaska; Groundfish Fisheries of the Bering Sea and Aleutian Islands Management Area*. National Oceanic and Atmospheric Administration 50 CFR Part 679, FR Doc No: E8-17144, Federal Register, 73, 144, https://www.govinfo.gov/content/pkg/FR-2008-07-25/html/E8-17144.htm

NOAA NMFS 2012. *Considerations for Research Planning in the Northern Bering Sea Research Area*. Agenda D-1 (d), NOAA NMFS Alaska Fisheries Science Center, North Pacific Fisheries Management Council, Achrorage, Alaska, USA, https://www.npfmc.org/wp-content/PDFdocuments/rural_outreach/NBSRA_DiscPap_912.pdf

Oksanen, J., Kindt, R., Legendre, P., O'Hara, B., Stevens, M.H.H., Oksanen, M.J. and Suggests, M. 2007. The vegan package. *Community ecology package, CRAN Repository*, **10**, 295, https://CRAN.R-project.org/package=vegan

Oliver, J., Slattery, P. and Connor, L.L. 1983. Walrus, *Odobenus rosmarus*, feeding in the Bering Sea: a benthic perspective. *Fishery Bulletin-National Oceanic and Atmospheric Administration*, **81**, 501–512, https://spo.nmfs.noaa.gov/content/walrus-odobenus-rosmarus-feeding-bering-sea-benthic-perspective

Petersen, M.R. and Douglas, D.C. 2004. Winter ecology of spectacled eiders: environmental characteristics and population change. *The Condor*, **106**, 79–94, https://doi.org/10.1650/7292

Petersen, M.R., Earned, W.W. and Douglas, D.C. 1999. At-sea distribution of spectacled eiders: a 120-year-old mystery resolved. *The Auk*, **116**, 1009–1020, https://doi.org/10.2307/4089681

Petersen, M.R., Grand, J.B. and Dau, C. 2000. Spectacled Eider (*Somateria Fischeri*), Version 2.0. *In*: Poole, A.F. and Gill, F. (eds) *The Birds of North America*. Cornell Lab of Ornithology, Ithaca, NY, https://doi.org/10.2173/bna.547

Pirtle-Levy, R. 2006. *A Shelf-to-Basin Examination of Food Supply for Arctic Benthic Macrofauna and the Potential Biases of Sampling Methodology*. Thesis, University of Tennessee – Knoxville, Knoxville, Tennessee, USA, https://trace.tennessee.edu/utk_grad thes/1764

Pohlert, T. 2020. Trend: Non-Parametric Trend Tests and Change-Point Detection. Package 'trend', CRAN Repository, 1.1.4, 37, https://CRAN.R-project.org/package=trend

Powell, E.N. and Mann, R. 2016. How well do we know the infaunal biomass of the continental shelf? *Continental Shelf Research*, **115**, 27–32, https://doi.org/10.1016/j.csr.2016.01.001

Powell, E.N., Kuykendall, K.M. and Moreno, P. 2017. The death assemblage as a marker for habitat and an indicator of climate change: Georges Bank, surfclams and ocean quahogs. *Continental Shelf Research*, **142**, 14–31, https://doi.org/10.1016/j.csr.2017.05.008

R Core Team and Contributors Worldwide 2022. R: The R Stats Package. CRAN Repository, 4.3.0, https://stat.ethz.ch/R-manual/R-devel/library/stats/html/00Index.html

Ray, G.C., McCormick-Ray, J., Berg, P. and Epstein, H.E. 2006. Pacific walrus: Benthic bioturbator of Beringia. *Journal of Experimental Marine Biology and Ecology*, **330**, 403–419, https://doi.org/10.1016/j.jembe.2005.12.043

Saupe, E.E., Hendricks, J.R., Portell, R.W., Dowsett, H.J., Haywood, A., Hunter, S.J. and Lieberman, B.S. 2014. Macroevolutionary consequences of profound climate change on niche evolution in marine molluscs over the past three million years. *Proceedings: Biological Sciences*, **281**, https://doi.org/10.1098/rspb.2014.1995

Siddon, E. 2021. *Ecosystem Status Report 2021 Eastern Bering Sea, Stock Assessment and Fishery Evaluation Report*. 2021 6, North Pacific Fishery Management Council, 1007 West Third, Suite 400, Anchorage, Alaska USA, https://apps-afsc.fisheries.noaa.gov/refm/docs/2021/EBSecosys.pdf

Staff, G.M. and Powell, E.N. 1999. Onshore–offshore trends in community structural attributes: death assemblages from the shallow continental shelf of Texas. *Continental Shelf Research*, **19**, 717–756, https://doi.org/10.1016/S0278-4343(98)00108-3

Stead, R.A. and Thompson, R.J. 2006. The influence of an intermittent food supply on the feeding behaviour of *Yoldia hyperborea* (Bivalvia: Nuculanidae). *Journal of Experimental Marine Biology and Ecology*, **332**, 37–48, https://doi.org/10.1016/j.jembe.2005.11.001

Steger, J., Bošnjak, M., Belmaker, J., Galil, B.S., Zuschin, M. and Albano, P.G. 2022. Non-indigenous molluscs in the Eastern Mediterranean have distinct traits and cannot replace historic ecosystem functioning. *Global Ecology and Biogeography*, **31**, 89–102, https://doi.org/10.1111/geb.13415

Todd, J. 2001. NMITA Molluscan Life Habits databases, https://fossils.its.uiowa.edu/database/molluscmollusclifestyles.htm

Tomašových, A. and Kidwell, S.M. 2009. Fidelity of variation in species composition and diversity partitioning by death assemblages: time-averaging transfers diversity from beta to alpha levels. *Paleobiology*, **35**, 94–118, https://doi.org/10.1666/08024.1

Tomašových, A. and Kidwell, S.M. 2011. Accounting for the effects of biological variability and temporal autocorrelation in assessing the preservation of species abundance. *Paleobiology*, **37**, 332–354, https://doi.org/10.1666/09506.1

Tomašových, A., Kidwell, S.M., Barber, R.F. and Kaufman, D.S. 2014. Long-term accumulation of carbonate shells reflects a 100-fold drop in loss rate. *Geology*, **42**, 819–822, https://doi.org/10.1130/g35694.1

Tomašových, A., Kidwell, S.M. and Barber, R. 2016. Inferring skeletal production from time-averaged assemblages: skeletal loss pulls the timing of production pulses towards the modern period. *Paleobiology*, **42**, 54–76, https://doi.org/10.1017/pab.2015.30

Tomašových, A., Gallmetzer, I., Haselmair, A., Kaufman, D., Kralj, M., Cassin, D. and Zuschin, M. 2018. Tracing the effects of eutrophication on molluscan communities in sediment cores: outbreaks of an opportunistic species coincide with reduced bioturbation and high frequency of hypoxia in the Adriatic Sea. *Paleobiology*, **44**, 575–602, https://doi.org/10.1017/pab.2018.22

Valentine, J.W., Jablonski, D., Kidwell, S. and Roy, K. 2006. Assessing the fidelity of the fossil record by using marine bivalves. *Proceedings of the National Academy of Sciences*, **103**, 6599–6604, https://doi.org/10.1073/pnas.0601264103

Vavrek, M.J. 2020. Fossil: palaeoecological and palaeogeographical analysis tools. Package 'fosil', CRAN Repository, 0.4.0, 47, https://CRAN.R-project.org/package=fossil

Weber, K. and Zuschin, M. 2013. Delta-associated molluscan life and death assemblages in the northern Adriatic Sea: implications for paleoecology, regional diversity and conservation. *Palaeogeography, Palaeoclimatology, Palaeoecology*, **370**, 77–91, https://doi.org/10.1016/j.palaeo.2012.11.021

Wickham, H., Chang, W. *et al*. 2022. ggplot2: Create Elegant Data Visualisations Using the Grammar of Graphics. Package 'ggplot2', CRAN Repository, 3.3.6, 292, https://CRAN.R-project.org/package= ggplot2

Yanes, Y. 2012. Anthropogenic effect recorded in the live–dead compositional fidelity of land snail assemblages from San Salvador Island, Bahamas. *Biodiversity and Conservation*, **21**, 3445–3466, https://doi.org/10.1007/s10531-012-0373-4